LOAN COPY: RETURN TO
AFSWC (SWOIL)
KIRTLAND AFB, NMEX

NACA
TN
3712
c.1

TECH LIBRARY KAFB, NM
0066330

NATIONAL ADVISORY COMMITTEE FOR AERONAUTICS

TECHNICAL NOTE 3712

BOUNDARY LAYER BEHIND SHOCK OR THIN EXPANSION WAVE MOVING INTO STATIONARY FLUID

By Harold Mirels

Lewis Flight Propulsion Laboratory
Cleveland, Ohio

Washington
May 1956

TECH LIBRARY KAFB, NM
0066330

TABLE OF CONTENTS

	Page
SUMMARY	1
INTRODUCTION	1
ANALYSIS	2
Coordinate Systems	2
Laminar Boundary Layer	3
Integral solution	9
Interpolation formulas	12
Wall surface temperature	15
Turbulent Boundary Layer	19
Boundary-layer solution	19
Wall surface temperature	24
CORRELATION OF DATA	26
CONCLUDING REMARKS	29
APPENDIXES	
A - SYMBOLS	30
B - WAVE RELATIONS	33
C - LAMINAR-BOUNDARY-LAYER SOLUTION REFERENCED TO A MEAN TEMPERATURE	36
D - EVALUATION OF I_N	38
REFERENCES	40

NATIONAL ADVISORY COMMITTEE FOR AERONAUTICS

TECHNICAL NOTE 3712

BOUNDARY LAYER BEHIND SHOCK OR THIN EXPANSION WAVE MOVING INTO STATIONARY FLUID

By Harold Mirels

3959

CT-1

SUMMARY

The boundary layer behind a shock or thin expansion wave advancing into a stationary fluid has been determined. Laminar and turbulent boundary layers were considered. The wall surface temperature behind the wave was also investigated. The assumption of a thin expansion wave is valid for weak expansions but becomes progressively less accurate for strong expansion waves.

The laminar-boundary-layer problem was solved by numerical integration except for the weak wave case, which can be solved analytically. Integral (Kármán-Pohlhausen type) solutions were also obtained to provide a guide for determining expressions which accurately represent the numerical data. Analytical expressions for various boundary-layer parameters are presented which agree with the numerical integrations within 1 percent.

The turbulent-boundary-layer problem was solved using integral methods similar to those employed for the solution of turbulent compressible flow over a semi-infinite flat plate. The fluid velocity, relative to the wall, was assumed to have a seventh-power profile. The Blasius equation, relating turbulent skin friction and boundary-layer thickness, was utilized in a form which accounted for compressibility.

Consideration of the heat transfer to the wall permitted the wall surface temperature, behind the wave, to be determined. The wall thickness was assumed to be greater than the wall thermal-boundary-layer thickness. It was found that the wall temperature was uniform (as a function of distance behind the wave) for the laminar-boundary-layer case but varied with distance for the turbulent-boundary-layer case.

INTRODUCTION

If a shock or expansion wave advances into a stationary fluid bounded by a wall, a boundary-layer flow is established along the wall behind the wave. This boundary-layer flow is often important in studies of phenomena

involving nonstationary waves (e.g., shock tube studies, initiation of detonation studies, etc.).

In references 1 to 3, the laminar boundary layer behind a shock wave is studied. The purpose of this paper is to extend reference 1 to include the case of thin expansion waves (i.e., expansion waves of zero thickness) and the case of turbulent boundary layers. This extension was motivated primarily by a desire to provide boundary-layer information for studies of shock attenuation in a shock tube (e.g., ref. 4). 3959

The assumption of a zero-thickness expansion wave (referred to as a "negative shock" in ref. 4) becomes progressively less accurate as the strength (pressure ratio) of the expansion wave increases. Thus, the applicability of the boundary-layer results in shock tubes wherein strong expansions occur may be questioned. Nevertheless, the assumption of a zero-thickness expansion wave will be retained for ranges of the parameter u_w/u_e (symbols defined in appendix A) corresponding to strong expansion waves. The reason for retaining the assumption is twofold. First, a qualitative estimate of the boundary layer in the constant-pressure region behind strong expansion waves is obtained. It may be possible to modify these results to give better agreement with more accurate estimates of the boundary layer behind a strong expansion wave. Second, the results are directly applicable to other physical problems such as (1) the boundary layer on a semi-infinite flat plate with tangential blowing and (2) the boundary layer behind a planar flame front propagating in a stationary combustible mixture.

An independent investigation of the boundary layer behind an expansion wave, taking into account the finite thickness of the expansion wave, is currently in progress at the NACA Langley laboratory.

ANALYSIS

A shock or expansion wave is considered to move with constant velocity, parallel to a wall, into a stationary fluid (fig. 1). The boundary layer along the wall behind the wave is to be determined. In the case of an expansion wave, finite thickness of the wave will be ignored. Both laminar and turbulent boundary layers will be considered.

Coordinate Systems

Let $\bar{x},\bar{y}$ be a coordinate system fixed with respect to the wall and let $\bar{u},\bar{v}$ be velocities parallel to $\bar{x},\bar{y}$ as indicated in figure 1(a). The flow is unsteady in the $\bar{x},\bar{y}$-coordinate system. Let x,y represent a coordinate system moving with the wave (fig. 1(b)). The velocities parallel to the x- and y-coordinates are denoted by u and v, respectively. In this coordinate system, the flow is steady.

Assume that at time $t = 0$ the two coordinate systems coincide. If $\bar{u}_d$ is the velocity of the wave relative to the wall, then $\bar{x}$ and x are related by $x = \bar{x} - \bar{u}_d t$. The axial velocities are related by $u = \bar{u} - \bar{u}_d$. Note that the wall moves with velocity $u_w = -\bar{u}_d$ in the x,y-coordinate system. The transformation relating the two systems can also be expressed as

$$\left.\begin{aligned} \bar{x} &= x - u_w t \\ \bar{y} &= y \\ \bar{u} &= u - u_w \\ \bar{v} &= v \end{aligned}\right\} \tag{1}$$

3959

CT-1 back

Equations defining conditions across the shock and expansion waves are summarized in appendix B.

Laminar Boundary Layer

The Prandtl boundary-layer equations apply for the flow in the vicinity of the wall, except at the base of the wave where the boundary-layer assumptions break down. By assuming laminar flow and $dp/dx = 0$, the boundary-layer equations for $x > 0$ are

$$\frac{\partial \rho u}{\partial x} + \frac{\partial \rho v}{\partial y} = 0 \tag{2a}$$

$$u \frac{\partial u}{\partial x} + v \frac{\partial u}{\partial y} = \frac{1}{\rho} \frac{\partial}{\partial y}\left(\mu \frac{\partial u}{\partial y}\right) \tag{2b}$$

$$\rho c_p\left(u \frac{\partial T}{\partial x} + v \frac{\partial T}{\partial y}\right) = \frac{\partial}{\partial y}\left(k \frac{\partial T}{\partial y}\right) + \mu\left(\frac{\partial u}{\partial y}\right)^2 \tag{2c}$$

$$p = \rho R T \tag{2d}$$

The boundary conditions for $x > 0$ are

$$\left.\begin{aligned} u(x,0) &= u_w & u(x,\infty) &= u_e \\ v(x,0) &= 0 & & \\ T(x,0) &= T_w & T(x,\infty) &= T_e \end{aligned}\right\} \tag{3}$$

These equations can be transformed to a form suitable for numerical integration. In accordance with reference 5, it will be assumed that μ and k are proportional to T and that c_p and σ are independent of T. These state properties will be defined to have the correct numerical values at the wall. The use of a mean reference temperature, rather than a wall reference temperature, is discussed in appendix C.

From equation (2a), a stream function ψ exists so that

3659

$$\left.\begin{aligned} \frac{\rho u}{\rho_w} &= \frac{\partial \psi}{\partial y} \\ \frac{\rho v}{\rho_w} &= -\frac{\partial \psi}{\partial x} \end{aligned}\right\} \tag{4}$$

Define a similarity parameter

$$\eta = \sqrt{\frac{u_e}{2x\nu_w}} \int_0^y \frac{T_w}{T(x,y)}\, dy \tag{5}$$

and assume that ψ can be expressed in the form

$$\psi = \sqrt{2u_e x \nu_w}\, f(\eta) \tag{6}$$

The velocities are then

$$\left.\begin{aligned} \frac{u}{u_e} &= f' \\ \frac{v}{u_e} &= -\frac{\rho_w}{\rho} \sqrt{\frac{\nu_w}{2xu_e}} \left(f + 2xf' \frac{\partial \eta}{\partial x}\right) \end{aligned}\right\} \tag{7}$$

Assume that μ and k are proportional to T and choose the constants of proportionality so that μ and k have the correct numerical values

at the wall; similarly, assume that c_p and σ are constant at their wall values. Thus,

3959

$$\left.\begin{aligned} \mu &= \frac{\mu_w}{T_w} T \\ k &= \frac{k_w}{T_w} T \\ c_p &= c_{p,w} \\ \sigma &= \sigma_w \end{aligned}\right\} \tag{8}$$

The momentum equation can now be written

$$\left.\begin{aligned} f''' + ff'' &= 0 \\ f(0) &= 0 \\ f'(0) &= u_w/u_e \\ f'(\infty) &= 1 \end{aligned}\right\} \tag{9}$$

and the energy equation becomes

$$\left.\begin{aligned} \left(\frac{T}{T_e}\right)'' + \sigma_w f\left(\frac{T}{T_e}\right)' &= -\frac{\sigma_w u_e^2}{c_{p,w} T_e} (f'')^2 \\ \frac{T(x,0)}{T_e} &= \frac{T_w}{T_e} \\ \frac{T(x,\infty)}{T_e} &= 1 \end{aligned}\right\} \tag{10}$$

Since equations (10) are linear, T can be expressed as the linear superposition of the solution for zero heat transfer plus the effect of heat transfer. That is,

$$\frac{T}{T_e} = 1 + \left(\frac{u_w}{u_e} - 1\right)^2 \frac{u_e^2 r(\eta)}{2T_e c_{p,w}} + \left(\frac{T_w}{T_e} - \frac{T_r}{T_e}\right) s(\eta) \tag{11}$$

where

$$\frac{T_r}{T_e} = 1 + \left(\frac{u_w}{u_e} - 1\right)^2 \frac{u_e^2 r(0)}{2T_e c_{p,w}} \tag{12}$$

and $r(\eta)$ and $s(\eta)$ are defined, respectively, by

$$\left.\begin{aligned} r'' + \sigma_w f r' &= \frac{-2\sigma_w}{\left(\frac{u_w}{u_e} - 1\right)^2} (f'')^2 \\ r(\infty) = r'(0) &= 0 \end{aligned}\right\} \tag{13}$$

3959

and

$$\left.\begin{aligned} s'' + \sigma_w f s' &= 0 \\ s(0) &= 1 \\ s(\infty) &= 0 \end{aligned}\right\} \tag{14}$$

Equations (13) and (14) can also be expressed in quadrature form:

$$\left.\begin{aligned} r &= \frac{2\sigma_w}{\left(\frac{u_w}{u_e} - 1\right)^2} \int_\eta^\infty \left[f''(\eta_2)\right]^{\sigma_w} d\eta_2 \int_0^{\eta_2} \left[f''(\eta_1)\right]^{2-\sigma_w} d\eta_1 \\ s &= \int_\eta^\infty \left[f''(\eta_1)\right]^{\sigma_w} d\eta_1 \Bigg/ \int_0^\infty \left[f''(\eta_1)\right]^{\sigma_w} d\eta_1 \end{aligned}\right\} \tag{15}$$

Boundary-layer parameters of interest may now be expressed as

$$\tau_w \equiv \left(\mu \frac{\partial u}{\partial y}\right)_w = u_e f''(0) \sqrt{\frac{u_e \rho_w \mu_w}{2x}} \tag{16a}$$

$$q_w \equiv \left(-k \frac{\partial T}{\partial y}\right)_w = -s'(0)(T_w - T_r) \sqrt{\frac{u_e \rho_w \mu_w}{2x}} \frac{c_{p,w}}{\sigma_w} \tag{16b}$$

$$\frac{v_e}{u_e} = \frac{\rho_w}{\rho_e}\sqrt{\frac{\nu_w}{2xu_e}}\left[\lim_{\eta\to\infty}(\eta - f) + \left(\frac{u_w}{u_e} - 1\right)^2 \frac{u_e^2}{2T_e c_{p,w}}\int_0^\infty r\,d\eta + \left(\frac{T_w}{T_e} - \frac{T_r}{T_e}\right)\int_0^\infty s\,d\eta\right] \tag{16c}$$

3959

$$\delta^* \equiv \int_0^x \frac{v_e}{u_e}\,dx = 2\,\frac{v_e}{u_e}\,x \tag{16d}$$

where q equals the heat transfer in the +y-direction. Equation (16d) results from the expression $v_e/u_e = d\delta^*/dx$, which can be deduced from the continuity equation and the definition of δ^*.

Equations (9) to (15) can be integrated analytically for $|u_w/u_e - 1| << 1$ (i.e., weak waves). The integrations were conducted in reference 1 and the results are summarized as follows:

$$f - \eta = \left\{\eta\,\mathrm{erfc}\left(\frac{\eta}{\sqrt{2}}\right) + \sqrt{\frac{2}{\pi}}\left[1 - \exp\left(-\frac{\eta^2}{2}\right)\right]\right\}\left(\frac{u_w}{u_e} - 1\right) + O\left(\frac{u_w}{u_e} - 1\right)^2 \tag{17a}$$

$$f' - 1 = \left[\mathrm{erfc}\left(\frac{\eta}{\sqrt{2}}\right)\right]\left(\frac{u_w}{u_e} - 1\right) + O\left(\frac{u_w}{u_e} - 1\right)^2 \tag{17b}$$

$$f'' = -\sqrt{\frac{2}{\pi}}\left(\frac{u_w}{u_e} - 1\right)e^{-\eta^2/2} + O\left(\frac{u_w}{u_e} - 1\right)^2 \tag{17c}$$

$$r = \frac{4}{\pi}\left(\frac{\sigma_w}{2 - \sigma_w}\right)^{1/2}\int_{\sin^{-1}\sqrt{\frac{\sigma_w}{2}}}^{\pi/2} \exp\left(\frac{-\sigma_w\eta^2}{2\sin^2\theta}\right)d\theta + O\left(\frac{u_w}{u_e} - 1\right) \tag{17d}$$

$$r(0) = \frac{4}{\pi}\left(\frac{\sigma_w}{2 - \sigma_w}\right)^{1/2}\left(\frac{\pi}{2} - \sin^{-1}\sqrt{\frac{\sigma_w}{2}}\right) + O\left(\frac{u_w}{u_e} - 1\right) \tag{17e}$$

$$\int_0^\infty r\,d\eta = \frac{2}{\sqrt{\pi}} + O\left(\frac{u_w}{u_e} - 1\right) \tag{17f}$$

$$s = \operatorname{erfc}\left(\sqrt{\frac{\sigma_w}{2}}\,\eta\right) + O\left(\frac{u_w}{u_e} - 1\right) \tag{17g}$$

$$s'(0) = -\sqrt{\frac{2\sigma_w}{\pi}} + O\left(\frac{u_w}{u_e} - 1\right) \tag{17h}$$

$$\int_0^\infty s\,d\eta = \sqrt{\frac{2}{\pi\sigma_w}} + O\left(\frac{u_w}{u_e} - 1\right) \tag{17i}$$

3959

Equations (15) are integrable for $\sigma_w = 1$. The results show

$$r = 1 - \left(\frac{\frac{u_w}{u_e} - f'}{\frac{u_w}{u_e} - 1}\right)^2 \tag{18a}$$

$$\int_0^\infty r\,d\eta = \lim_{\eta\to\infty}\left[\frac{\left(2\,\frac{u_w}{u_e} - 1\right)(f - \eta) + f''(0)}{\left(\frac{u_w}{u_e} - 1\right)^2}\right] \tag{18b}$$

$$s = \frac{f' - 1}{\frac{u_w}{u_e} - 1} \tag{18c}$$

$$\int_0^\infty s\,d\eta = \lim_{\eta\to\infty}\left(\frac{f - \eta}{\frac{u_w}{u_e} - 1}\right) \tag{18d}$$

Equations (9) have been integrated numerically (using an IBM card-programmed electronic calculator) for $u_w/u_e = 1.5, 2, 3, 4, 5$, and 6, and the results are presented in reference 1. The range $1 \leq u_w/u_e \leq 6$

covers the entire range from very weak to very strong shock waves. Equations (15) are also evaluated in reference 1 for $\sigma_w = 0.72$ and $u_w/u_e = 2$, 4, and 6. In order to extend the numerical calculations to the case of a thin expansion wave, equations (9) have been integrated for $u_w/u_e = 0$, 0.25, 0.50, and 0.75 (table I). The case $u_w/u_e = 0$ is the well-known Blasius problem for flow past a semi-infinite flat plate and is included herein for the sake of completeness. Equations (15) were integrated for $u_w/u_e = 0$, 0.25, 0.50, 0.75 and $\sigma_w = 0.72$ (table I). From appendix B, the limiting value of u_w/u_e for strong expansion waves is $\frac{u_w}{u_e} = \frac{\gamma - 1}{\gamma + 1}$. These calculations were made using the integration technique described in appendix B of reference 6. The results of reference 1 for $u_w/u_e = 2$, 4, and 6 are also included in table I.

3959

CT-2

Integral solution. - The numerical integrations of equations (9) and (15) have the limitation that only specific values of u_w/u_e and σ_w can be treated. The analytic dependence of the boundary-layer parameters on u_w/u_e and σ_w are not explicitly defined by these specific solutions. In order to obtain approximate analytic solutions, an integral (Kármán-Pohlhausen) method of approach will now be used. The results will be used later in this section to obtain analytic expressions which accurately represent the numerical data presented in table I of this report.

Integrating equations (9) with respect to η, in the range $0 \leqslant \eta \leqslant \infty$, gives the integral form of the momentum equation

$$f''(0) = \int_0^\infty f'(1 - f')d\eta \tag{19}$$

Let $y = \tilde{\delta}$ be the edge of the boundary layer from a Pohlhausen point of view. The corresponding value of η is designated $\eta_{\tilde{\delta}}$. Define $\zeta \equiv \eta/\eta_{\tilde{\delta}}$. The velocity f' is now represented by a fourth-degree polynomial in ζ in the range $0 \leqslant \zeta \leqslant 1$.[1] Using the two boundary conditions on f' noted in equations (9) plus the boundary conditions $(f''')_{\zeta=0} = 0$, in order to satisfy equations (9), and

[1]References 3 and 7 also used integral approaches employing fourth-degree polynomials in studies of the laminar boundary layer behind moving shocks. In reference 8, a normalized error function was used instead of the fourth-degree polynomial. This resulted in very good agreement with the exact numerical integration of the corresponding boundary-layer equations.

$(f'')_{\zeta=1} = (f''')_{\zeta=1} = 0$, in order to get a smooth joining with the external flow, gives

$$\left.\begin{aligned} &\text{for } 0 \leqslant \zeta \leqslant 1, \\ &\qquad f' = \frac{u_w}{u_e} - \left(\frac{u_w}{u_e} - 1\right)\left(2\zeta - 2\zeta^3 + \zeta^4\right) \\ &\text{for } 1 < \zeta, \\ &\qquad f' = 1 \end{aligned}\right\} \tag{20}$$

3959

Equation (19) can be written as

$$f''(0) = \eta_{\tilde{\delta}} \int_0^1 f'(1 - f')d\zeta \quad . \tag{21}$$

Substituting equations (20) into equation (21), noting $f''(0) = \frac{2}{\eta_{\tilde{\delta}}}\left(1 - \frac{u_w}{u_e}\right)$ gives

$$\eta_{\tilde{\delta}} = 2\sqrt{\frac{315}{74 + 115\frac{u_w}{u_e}}} \tag{22}$$

which, together with equations (20), defines f'. The following quantities are of interest:

$$f''(0) = \left(1 - \frac{u_w}{u_e}\right)\sqrt{\frac{74 + 115\frac{u_w}{u_e}}{315}} \tag{23a}$$

$$\lim_{\eta\to\infty} (\eta - f) \equiv \int_0^\infty (1 - f')d\eta$$

$$= \frac{6}{10}\left(1 - \frac{u_w}{u_e}\right)\sqrt{\frac{315}{74 + 115\frac{u_w}{u_e}}} \tag{23b}$$

Equations (23) are compared, in table II, with the exact integration of equations (9) for $u_w/u_e = 0$, 1, and 6. It is seen that equation (23a)

agrees within 4 percent with the exact integration. Equation (23b) agrees within 2 percent at $u_w/u_e = 0$ and within 10 percent at $u_w/u_e = 6$. Table II serves to indicate the accuracy of the integral method of solution of the momentum equation.

Substitution of equations (20) and (22) into equations (15) gives

$$r = G(\sigma_w, \zeta) \tag{24a}$$

$$s = H(\sigma_w, \zeta) \tag{24b}$$

$$\int_0^\infty r \, d\eta = \eta_{\tilde{\delta}} I(\sigma_w) \tag{24c}$$

$$\int_0^\infty s \, d\eta = \eta_{\tilde{\delta}} J(\sigma_w) \tag{24d}$$

$$s'(0) = K(\sigma_w)/\eta_{\tilde{\delta}} \tag{24e}$$

where

$$F(\zeta) \equiv (1 - \zeta)^2(2\zeta + 1) \tag{25a}$$

$$G(\sigma_w, \zeta) \equiv 8\sigma_w \int_\zeta^1 \left[F(\zeta_2)\right]^{\sigma_w} d\zeta_2 \int_0^{\zeta_2} \left[F(\zeta_1)\right]^{2-\sigma_w} d\zeta_1 \tag{25b}$$

$$H(\sigma_w, \zeta) \equiv \int_\zeta^1 \left[F(\zeta_1)\right]^{\sigma_w} d\zeta_1 \Big/ \int_0^1 \left[F(\zeta_1)\right]^{\sigma_w} d\zeta_1 \tag{25c}$$

$$I(\sigma_w) \equiv \int_0^1 G(\sigma_w, \zeta) d\zeta \tag{25d}$$

$$J(\sigma_w) \equiv \int_0^1 H(\sigma_w, \zeta) d\zeta \tag{25e}$$

$$K(\sigma_w) \equiv -1 \Big/ \int_0^1 \left[F(\zeta_1)\right]^{\sigma_w} d\zeta_1 \tag{25f}$$

3959

CT-2 back

Equations (24) define the functional dependence, on σ_w, ζ and u_w/u_e, of the various quantities noted to within the accuracy of the integral method. Equations (25) can be integrated analytically for $\sigma_w = 1$. For other Prandtl numbers, numerical integrations, or approximate analytical integrations would be required.

Equations (24c) to (24e) indicate that the functional dependence of $\int_0^\infty r\,d\eta$, $\int_0^\infty s\,d\eta$, and $s'(0)$ on σ_w is independent of u_w/u_e. 3959
Comparison of equation (24d) with the exact solution for $s'(0)$ at $u_w/u_e = 1$ (i.e., eq. (17h)) indicates that $K(\sigma_w)$ should be proportional to $\sigma_w^{1/2}$. However, comparison of equation (24d) with the exact solution tion for $u_w/u_e = 0$ (ref. 5) indicates that $K(\sigma_w)$ should be proportional to $\sigma_w^{1/3}$ for σ_w in the range $0.6 < \sigma_w < 1$. The discrepancy is due to to limitations of the integral method. Hence equations (24) and (25) would have to be modified if greater accuracy is desired. Possible modifications are indicated in the next section. Comparison of equations (24c) and (24d) with equations (17f) and (17i) indicates that, for u_w/u_e near 1, $I(\sigma_w)$ is a constant while $J(\sigma_w)$ varies directly as $1/\sqrt{\sigma_w}$.

Interpolation formulas. - Equations (23) and (24) can be used as a guide to obtain analytic expressions which accurately represent the data obtained from the exact numerical integrations of equations (9) and (15). The various boundary-layer parameters are assumed to depend on u_w/u_e and σ_w as follows:

$$\frac{f''(0)}{1 - \frac{u_w}{u_e}} = C_1\sqrt{1 + C_2\frac{u_w}{u_e}} \tag{26a}$$

$$\lim_{\eta\to\infty}\frac{\eta - f}{1 - \frac{u_w}{u_e}} = \frac{C_3}{\sqrt{1 + C_4\frac{u_w}{u_e}}} \tag{26b}$$

$$\int_0^\infty r\,d\eta = \frac{C_5}{\sqrt{1 + C_6\frac{u_w}{u_e}}}(\sigma_w)^{D_5+D_6(u_w/u_e)} \tag{26c}$$

3959

$$\int_0^\infty s\,d\eta = \frac{C_7}{\sqrt{1 + C_8 \frac{u_w}{u_e}}} (\sigma_w)^{D_7+D_8(u_w/u_e)} \tag{26d}$$

$$s'(0) = C_9 \sqrt{1 + C_{10} \frac{u_w}{u_e}} (\sigma_w)^{D_9+D_{10}(u_w/u_e)} \tag{26e}$$

$$r(0) = (\sigma_w)^{D_{11}+D_{12}(u_w/u_e)} \tag{26f}$$

The case of an expansion wave and a shock wave are distinguished by writing separate formulas for the ranges $0 \leqslant u_w/u_e \leqslant 1$ and $1 \leqslant u_w/u_e \leqslant 6$. The results are,

for $0 \leqslant u_w/u_e \leqslant 1$,

$$\frac{f''(0)}{1 - \frac{u_w}{u_e}} = 0.470 \sqrt{1 + 1.887 \frac{u_w}{u_e}} \tag{27a}$$

$$\lim_{\eta \to \infty} \frac{\eta - f}{1 - \frac{u_w}{u_e}} = \frac{1.217}{\sqrt{1 + 1.326 \frac{u_w}{u_e}}} \tag{27b}$$

$$\int_0^\infty r\,d\eta = \frac{1.686}{\sqrt{1 + 1.234 \frac{u_w}{u_e}}} (\sigma_w)^{0.22(1-u_w/u_e)} \tag{27c}$$

$$\int_0^\infty s\,d\eta = \frac{1.217}{\sqrt{1 + 1.326 \frac{u_w}{u_e}}} (\sigma_w)^{-0.36-0.14(u_w/u_e)} \tag{27d}$$

$$s'(0) = -0.470 \sqrt{1 + 1.887 \frac{u_w}{u_e}} (\sigma_w)^{0.35+0.15(u_w/u_e)} \tag{27e}$$

$$r(0) = (\sigma_w)^{0.50-0.13(u_w/u_e)} \tag{27f}$$

for $1 \leqslant (u_w/u_e) \leqslant 6$,

$$\frac{f''(0)}{1 - \frac{u_w}{u_e}} = 0.489 \sqrt{1 + 1.665 \frac{u_w}{u_e}} \tag{27a'}$$

$$\lim_{\eta \to \infty} \frac{\eta - f}{1 - \frac{u_w}{u_e}} = \frac{1.135}{\sqrt{1 + 1.022 \frac{u_w}{u_e}}} \tag{27b'}$$

3959

$$\int_0^\infty r \, d\eta = \frac{1.569}{\sqrt{1 + 0.933 \frac{u_w}{u_e}}} (\sigma_w)^{0.045(1-u_w/u_e)} \tag{27c'}$$

$$\int_0^\infty s \, d\eta = \frac{1.134}{\sqrt{1 + 1.022 \frac{u_w}{u_e}}} (\sigma_w)^{-0.47-0.029(u_w/u_e)} \tag{27d'}$$

$$s'(0) = -0.489 \sqrt{1 + 1.664 \frac{u_w}{u_e}} (\sigma_w)^{0.48+0.022(u_w/u_e)} \tag{27e'}$$

$$r(0) = (\sigma_w)^{0.39-0.023(u_w/u_e)} \tag{27f'}$$

Equations (27) were obtained by matching equations (26), at the end points of the intervals $0 \leqslant (u_w/u_e) \leqslant 1$ and $1 \leqslant (u_w/u_e) \leqslant 6$, with the exact integrations of equations (9) and (15) (table I). Equations (27) agree with table I to within 1 percent. The accuracy of equations (27) can be estimated from table III, which compares equations (27) with table I for the intermediate points $u_w/u_e = 0.25$, 0.50, 0.75, 2, and 4.

Equations (27) are based on numerical solutions corresponding to $\sigma_w = 1$ and $\sigma_w = 0.72$. They should give reasonable estimates for other values of σ_w of this order (i.e., $0.6 \leqslant \sigma_w \leqslant 1$). An exact appraisal of equations (27) for σ_w other than 1 and 0.72 requires further investigation of the exact integrations of equations (9) and (15). Such an investigation is considered beyond the scope of this report.

Wall surface temperature. - Until now it has been assumed that the wall surface temperature is constant behind the shock or expansion wave. This can be shown to be true for a laminar boundary layer. The magnitude of the wall temperature will now be determined, assuming that the wall thickness is greater than the wall thermal boundary layer.[2]

In the steady x,y-coordinate system, the wall has a uniform velocity u_w. However, there is a thermal boundary layer in the wall which is similar to that in the adjacent fluid (fig. 2). Assume that before
3959 the appearance of the wave, the fluid and the wall were in thermal equilibrium at the temperature T_b.

When a quantity is discontinuous across $y = 0$, the subscripts w and 0^- will be used to indicate quantities evaluated at $y = 0^+$ and $y = 0^-$, respectively. Neglect the variation of state properties (such as k, ρ, etc.) in the wall and write the diffusivity of the wall as $\alpha_{0^-} \equiv \left(\frac{k}{\rho c_p}\right)_{0^-}$. By using boundary-layer assumptions, the energy equation for the wall becomes

$$\frac{\partial T}{\partial x} = \frac{\alpha_{0^-}}{u_w} \frac{\partial^2 T}{\partial y^2} \tag{28a}$$

with the boundary conditions, for $x > 0$,

$$\left.\begin{aligned} T(x,0) &= T_w \\ T(x,-\infty) &= T_b \end{aligned}\right\} \tag{28b}$$

Equation (28a) can be obtained from equation (2c) by assuming the wall to be equivalent to a fluid with $\mu = v = 0$. Assume (to be verified later in this section) that T_w is constant. The solution of equations (28) is then

$$\frac{T_w - T}{T_w - T_b} = \operatorname{erf}\left(\frac{-y}{2\sqrt{(x\alpha_{0^-})/u_w}}\right) \tag{29}$$

---

[2]The problem of the wall surface temperature associated with the laminar boundary layer behind a moving shock was solved, independently, in reference 8. The development in reference 8 is somewhat more detailed than that given herein. The results are essentially in agreement with this report.

The heat transfer in the +y-direction at $y = 0^-$ is

$$q_{0^-} \equiv \left(-k \frac{\partial T}{\partial y}\right)_{0^-}$$

$$= \frac{(T_b - T_w)k_{0^-}}{\sqrt{(\pi x \alpha_{0^-})/u_w}} \tag{30}$$

3959

From equation (16b), the heat transferred into the fluid is

$$q_w = -s'(0)(T_w - T_r)\sqrt{\frac{u_e \rho_w \mu_w}{2x}}\left(\frac{c_{p,w}}{\sigma_w}\right) \tag{31}$$

Equations (30) and (31) may be equated, yielding

$$\frac{T_w - T_b}{T_b} = A\,\frac{\left[(T_r/T_b) - 1\right]}{1 + A}$$

$$= A\left(\frac{T_r}{T_b} - 1\right) + O(A^2) \tag{32a}$$

where

$$A = \frac{-s'(0)}{\sqrt{\frac{2}{\pi}\,\sigma_w}}\sqrt{\frac{u_e}{u_w}}\sqrt{\frac{\alpha_{0^-}}{\alpha_w}}\,\frac{k_w}{k_{0^-}} \tag{32b}$$

Equation (32a) is solved for T_w by iteration (since A and T_r are functions of T_w). The choice $T_w = T_b$, to start the iteration, is a good first approximation. Note that T_w is a constant, which is consistent with and, therefore, substantiates the original assumption to this effect.

The ratio T_r/T_b can be expressed as a function of u_w/u_e and $r(0)$ by use of equation (12) and equations (B3), (B4), (B7), and (B8) of appendix B. The results are (assuming $c_{p,e} = c_{p,w}$)

for $u_w/u_e > 1$,

$$\frac{T_r}{T_b} - 1 = \left(\frac{u_w}{u_e} - 1\right)\left[\frac{\left(\frac{u_w}{u_e} + 1\right) + \left(\frac{u_w}{u_e} - 1\right) r(0)}{\frac{u_w}{u_e}\left(\frac{\gamma + 1}{\gamma - 1} - \frac{u_w}{u_e}\right)}\right] \tag{33a}$$

$$= 2\,\frac{\frac{u_w}{u_e} - 1}{6 - \frac{u_w}{u_e}} = \frac{1}{3}\left(M_b^2 - 1\right) \qquad \text{for } \gamma = 1.4;\ r(0) = 1$$

3959

for $u_w/u_e < 1$,

CT-3

$$\frac{T_r}{T_b} - 1 = \left(\frac{\gamma - 1}{2u_w/u_e}\right)^2\left[\left(\frac{\gamma + 1}{\gamma - 1}\frac{u_w}{u_e} - 1\right)^2 + \frac{2}{\gamma - 1} r(0)\left(\frac{u_w}{u_e} - 1\right)^2\right] - 1 \tag{33b}$$

$$\left.\begin{aligned} &= -\frac{2\left[8(u_w/u_e) - 3\right](1 - u_w/u_e)}{25(u_w/u_e)^2} \\ &= -2\left[3\left(\frac{p_e}{p_b}\right)^{1/7} - 2\right]\left[1 - \left(\frac{p_e}{p_b}\right)^{1/7}\right] \end{aligned}\right\} \text{for } \gamma = 1.4;\ r(0) = 1$$

It should be noted that for $T_r/T_b > 1$ the heat transfer is from the fluid to the wall, whereas for $T_r/T_b < 1$ the heat transfer is from the wall to the fluid. Thus, for the flow behind a shock wave (eq. (33a)) the heat transfer is always from the fluid to the wall. However, for the flow behind an expansion wave (eq. (33b)) the heat transfer is from the wall to the fluid for relatively weak expansion waves and from the fluid to the wall for strong expansion waves. When $\gamma = 1.4$ and $r(0) = 1$, the change in the direction of heat transfer occurs at $p_e/p_b = (2/3)^7$. This change in heat-transfer direction is a consequence of the fact that the stagnation temperature (relative to the wall) behind a thin expansion wave is less than T_b for $p_e/p_b > \left(\frac{3 - \gamma}{\gamma + 1}\right)^{\frac{2\gamma}{\gamma - 1}}$ and is greater than T_b for $p_e/p_b < \left(\frac{3 - \gamma}{\gamma + 1}\right)^{\frac{2\gamma}{\gamma - 1}}$. The boundary-layer recovery temperature T_r

equals the free-stream stagnation temperature (relative to the wall) for $r(0) = 1$ and is somewhat less than the stagnation temperature for $r(0) < 1$. If the finite thickness of the wave is taken into account for a very strong expansion wave, it is expected that the heat transfer will be from the wall to the fluid for the early stages of the expansion and from the fluid to the wall for the final stages of the expansion.

The order of magnitude of $(T_w - T_b)/T_b$ will now be determined. Equations (17h), (27e), and (27e') indicate $-s'(0)\sqrt{\frac{\pi}{2\sigma_w}}\sqrt{\frac{u_e}{u_w}} \cong 1$. Therefore, A can be approximated as 3959

$$A \cong \sqrt{\frac{\alpha_{0-}}{\alpha_w}}\,\frac{k_w}{k_{0-}} \tag{34}$$

If k is proportional to T and c_p is constant, then the value of $k/\sqrt{\alpha}$ is independent of temperature for a given gas. Assume the fluid to be air and the wall to be cast iron (carbon, approx. 4 percent) both initially at a temperature $T_b = 530^\circ$ R. Using the property values of reference 9 evaluated at 530° R gives $A \cong 0.0004$. Substituting equations (33) into equation (32a) yields, with $A = 0.0004$, $r(0) = 1$, and $\gamma = 1.4$,

for $u_w/u_e > 1$,

$$\frac{T_w - T_b}{T_b} \cong 0.0004\left(\frac{M_b^2 - 1}{3}\right) \tag{35a}$$

for $u_w/u_e < 1$,

$$\frac{T_w - T_b}{T_b} \cong -0.0008\left[3\left(\frac{p_e}{p_b}\right)^{1/7} - 2\right]\left[1 - \left(\frac{p_e}{p_b}\right)^{1/7}\right] \tag{35b}$$

The wall will remain within 0.1 percent of its original temperature for shocks up to $M_b \cong 3$ and for all expansion waves. The wall will remain within 1 percent of its original value for shocks up to $M_b \cong 9$ and within 10 percent of its original value for $M_b \cong 27$. Similar results would be obtained if other gases and wall metals are used. The important parameter k_w/k_{0-} is small because of the relatively low heat conductivity of gases compared with metals. The fact that the wall remains essentially at its original temperature (except possibly for extremely strong shock waves) justifies the disregard of the variation of wall state properties with temperatures in equation (28a).

The thickness of the wall thermal boundary layer Δ_T can readily be found. Define the edge of the thermal boundary layer to correspond with $(T_w - T)/(T_w - T_b) = 0.99$. Then, from equation (29),

$$\Delta_T = 3.6\sqrt{x\alpha_{0-}/u_w} \tag{36}$$

It is of interest to compare Δ_T with the thermal-boundary-layer thickness in the fluid δ_T. For convenience, consider the case of weak waves. Equations (11) and (17g), together with the previously defined criterion for the edge of a thermal boundary layer, give

$$\delta_T = 3.6\sqrt{\frac{x\alpha_w}{u_w}}\left[1 + O(u_w/u_e - 1)\right] \tag{37}$$

Then

$$\frac{\Delta_T}{\delta_T} = \sqrt{\frac{\alpha_{0-}}{\alpha_w}}\left[1 + O(u_w/u_e - 1)\right] \tag{38}$$

which is of the order of 1 for some air and metal wall combinations.

The solution for the wall surface temperature presented herein is valid provided the wall thickness is (at least) greater than Δ_T.

Turbulent Boundary Layer

Previously, it was assumed that the boundary layer behind the wave was laminar. Now the turbulent-boundary-layer case will be treated using integral methods. The solutions will be obtained by extending empirical, semi-infinite flat-plate, boundary-layer data to the case where the wall is moving.

Boundary-layer solution. - The integral form of the momentum equation is

$$\begin{aligned}\frac{\tau_w}{\rho_e u_e^2} &= \frac{d}{dx}\int_0^\infty \frac{\rho u}{\rho_e u_e}\left(1 - \frac{u}{u_e}\right) dy \\ &= \frac{d\theta}{dx}\end{aligned} \tag{39}$$

where u/u_e represents the average velocity. As before, denote the boundary-layer thickness by $\tilde{\delta}$ and define a similarity parameter

3959

CT-3 back

$\zeta_T = y/\tilde{\delta}$. It is necessary to express u/u_e as a function of ζ_T. In studies of the turbulent boundary layer on a semi-infinite flat plate, it is customary to assume $u/u_e = \zeta_T^{1/7}$ for $0 \leqslant \zeta_T \leqslant 1$. The use of the seventh-power law appears to agree with available data, even for high Mach number flows, and to result in reasonably accurate relations for skin friction (e.g., refs. 10 and 11). In order to extend this profile to the case of a moving wall, it is assumed that the fluid velocities relative to the wall have a seventh-power profile. That is, 3959

$$\left.\begin{aligned} &\text{for } 0 \leqslant \zeta_T \leqslant 1, \\ &\qquad \left|\frac{u - u_w}{u_e - u_w}\right| = \zeta_T^{1/7} \\ &\text{for } 1 \leqslant \zeta_T, \\ &\qquad \left|\frac{u - u_w}{u_e - u_w}\right| = 1 \end{aligned}\right\} \tag{40}$$

It is also necessary to express T/T_e $(= \rho_e/\rho)$ as a function of ζ_T. The form assumed herein is

$$\left.\begin{aligned} &\text{for } 0 \leqslant \zeta_T \leqslant 1, \\ &\qquad \frac{\rho_e}{\rho} = \frac{T}{T_e} = \frac{T_w}{T_e}\left(1 + b\zeta_T^{1/7} - c\zeta_T^{2/7}\right) \\ &\text{for } 1 \leqslant \zeta_T, \\ &\qquad \frac{\rho_e}{\rho} = \frac{T}{T_e} = 1 \end{aligned}\right\} \tag{41}$$

where

$$b = \frac{T_r}{T_w} - 1$$

$$c = \left(\frac{T_r}{T_e} - 1\right)\frac{T_e}{T_w}$$

For a Prandtl number of 1, the dependence of T/T_e on u/u_e in equations (41) is the same as that indicated in equation (12). When the Prandtl number is not too far from 1, equations (41) should give at least a reasonable estimate for T/T_e.

By using equations (40) and (41), the boundary-layer momentum thickness and displacement thickness can be expressed as

$$\frac{\theta}{\tilde{\delta}} = 7\,\frac{T_e}{T_w}\left(1 - \frac{u_w}{u_e}\right)\left[\frac{u_w}{u_e}\,I_6 + \left(1 - 2\,\frac{u_w}{u_e}\right)I_7 - \left(1 - \frac{u_w}{u_e}\right)I_8\right] \tag{42a}$$

$$\frac{\delta^*}{\tilde{\delta}} = 1 - 7\,\frac{T_e}{T_w}\left[\frac{u_w}{u_e}\,I_6 + \left(1 - \frac{u_w}{u_e}\right)I_7\right] \tag{42b}$$

3959

where I_6, I_7, and I_8 are functions of b and c defined by the integral

$$I_N = \int_0^1 \frac{z^N dz}{1 + bz - cz^2} \tag{43}$$

with $N = 6$, 7, or 8. A method for evaluating I_N is indicated in appendix D. It should be noted that the integrals I_7 and $(I_7 - I_8)$ are tabulated in reference 11 for the range $-1 < b \leqslant 10$ and $0 \leqslant \frac{c}{b + 1} < 1$. The results were computed using Simpson's rule. The results of reference 11 can be used to tabulate values of I_8 and I_6. The integral I_6 is found from the relation $I_6 = \frac{1}{7} - bI_7 + cI_8$, which follows from equation (43). The reciprocals of I_6, I_7, and I_8, based on the data of reference 11, are presented in table IV. Reciprocals are used to permit linear interpolation. When b is near -1 or $c/(b + 1)$ is near 1, the linear interpolation becomes inaccurate and use of appendix D is recommended.

Since $\theta/\tilde{\delta}$ is independent of x (assuming the wall temperature to be constant), equation (39) can be written

$$\frac{\tau_w}{\rho_e u_e^2} = \frac{\theta}{\tilde{\delta}}\,\frac{d\tilde{\delta}}{dx} \tag{44}$$

In order to integrate equation (44), it is necessary to have a relation between τ_w and $\tilde{\delta}$. For incompressible turbulent flow past a semi-infinite flat plate, the Blasius relation (ref. 12) is

$$\frac{\tau_w}{\rho_e u_e^2} = 0.0225\left(\frac{\nu_e}{u_e\tilde{\delta}}\right)^{1/4} \tag{45}$$

This formula can be extended to approximate the compressible flow over a semi-infinite plate by evaluating the fluid properties at a suitable mean temperature T_m (refs. 10, 11, and 13) giving

$$\frac{\tau_w}{\rho_m u_e^2} = 0.0225 \left(\frac{\nu_m}{u_e \tilde{\delta}}\right)^{1/4} \tag{46a}$$

or

$$\frac{\tau_w}{\rho_e u_e^2} = 0.0225\ \varphi \left(\frac{\nu_e}{u_e \tilde{\delta}}\right)^{1/4} \tag{46b}$$

3959

where

$$\varphi = \left(\frac{\mu_m}{\mu_e}\right)^{1/4} \left(\frac{T_e}{T_m}\right)^{3/4}$$

From reference 13, a reasonable estimate for T_m is

$$T_m = 0.5(T_w + T_e) + 0.22(T_r - T_e) \tag{47}$$

When the wall is moving, the logical extension of equation (46b) is to use velocities relative to the wall. Thus,

$$\frac{\tau_w}{\rho_e (u_e - u_w)^2} = 0.0225\ \varphi \left(\frac{\nu_e}{|u_e - u_w| \tilde{\delta}}\right)^{1/4} \frac{u_e - u_w}{|u_e - u_w|} \tag{48a}$$

or

$$\frac{\tau_w}{\rho_e u_e^2} = 0.0225\ \varphi \left(1 - \frac{u_w}{u_e}\right) \left|1 - \frac{u_w}{u_e}\right|^{3/4} \left(\frac{\nu_e}{u_e \tilde{\delta}}\right)^{1/4} \tag{48b}$$

Equations (48) are expressed, as indicated to ensure that τ_w has the same sign as $u_e - u_w$, which is to be expected from physical considerations. Substitution of equation (48b) into equation (44) permits the latter to be integrated, for T_w constant, giving

$$\tilde{\delta} = 0.0574 \left(\varphi \frac{1 - u_w/u_e}{\theta/\tilde{\delta}}\right)^{4/5} \left|1 - u_w/u_e\right|^{3/5} \left(\frac{\nu_e}{u_e x}\right)^{1/5} x \tag{49}$$

Other boundary-layer parameters of interest are

$$\frac{\tau_w}{\rho_e u_e^2} = 0.0460\,\frac{\theta}{\tilde{\delta}}\left(\varphi\,\frac{1 - u_w/u_e}{\theta/\tilde{\delta}}\right)^{4/5}\left|1 - u_w/u_e\right|^{3/5}\left(\frac{\nu_e}{u_e x}\right)^{1/5} \tag{50a}$$

3959

$$\frac{v_e}{u_e} = \frac{d\delta^*}{dx}$$

$$= 0.0460\,\frac{\delta^*}{\tilde{\delta}}\left(\varphi\,\frac{1 - u_w/u_e}{\theta/\tilde{\delta}}\right)^{4/5}\left|1 - u_w/u_e\right|^{3/5}\left(\frac{\nu_e}{u_e x}\right)^{1/5} \tag{50b}$$

The heat transfer at the wall can be estimated using a Reynolds analogy. For compressible flow over a semi-infinite flat plate, the Reynolds analogy may be expressed as (ref. 13)

$$q_w = \frac{c_{p,m}(T_w - T_r)}{u_e}\,\sigma_m^{-2/3}\,\tau_w \tag{51}$$

When the wall moves, an estimate of the heat transfer might be obtained from

$$q_w = \frac{c_{p,m}(T_w - T_r)\sigma_m^{-2/3}}{u_e - u_w}\,\tau_w \tag{52}$$

It is pointed out in the CORRELATION OF DATA section that the exponent of σ_m should probably decrease in magnitude with increasing u_w/u_e.

The recovery temperature T_r is yet to be determined. By analogy with the turbulent flow over a semi-infinite flat plate, T_r may be estimated as (ref. 13)

$$\frac{T_r}{T_e} = 1 + \left(\frac{u_w}{u_e} - 1\right)^2 \frac{u_e^2 r(0)}{2T_e c_{p,m}} \tag{53a}$$

where

$$r(0) \cong \sqrt[3]{\sigma_m} \tag{53b}$$

Equation (53a) is solved by iteration since $c_{p,m}$ and $r(0)$ are functions of T_r. For the laminar-boundary-layer case, $r(0)$ increased with

an increase in u_w/u_e. This suggests that equation (53b) might underestimate $r(0)$ at the higher values of u_w/u_e. However, equation (53b) is probably well within the accuracy of the other assumptions required to solve the turbulent-boundary-layer equations.

Wall surface temperature. - For convenience, it was assumed during the course of the turbulent-boundary-layer solution that the wall surface temperature was constant with x. The validity of this assumption can be investigated by solving for the wall temperature as was done for the laminar boundary layer. 3959

Equating equations (52) and (30), plus equation (48b), gives

$$\frac{T_w - T_b}{T_b} = \frac{B[(T_r/T_b) - 1]}{1 + B}$$

$$= B\left(\frac{T_r}{T_b} - 1\right) + O(B^2) \tag{54}$$

where

$$B = 0.0815\,\varphi^{4/5}\,\frac{c_{p,m}}{c_{p,e}}\left(\frac{\sigma_m}{\sigma_e}\right)^{-2/3}\sigma_e^{-1/6}\left(\frac{\theta/\delta^*}{1 - u_w/u_e}\right)^{1/5}\left|1 - u_w/u_e\right|^{3/5}\sqrt{\frac{u_e}{u_w}}\left(\sqrt{\frac{\alpha_0}{\alpha_e}}\,\frac{k_e}{k_0}\right)\left(\frac{xu_e}{\nu_e}\right)^{3/10}$$

Unlike the laminar-boundary-layer case, B varies with x. Therefore, T_w/T_b varies with x, which contradicts the original assumptions under which equations (54) were derived. However, equations (54) can be used to establish the conditions under which T_w is nearly equal to T_b. The procedure to follow is to evaluate the right side of equations (54) assuming $T_w = T_b$. (Eqs. (33) are applicable.) If the resulting value for $(T_w - T_b)/T_b$ is small (e.g., less than 0.1 for all values of x under consideration), then the assumption of a constant wall temperature is reasonably accurate and the solution indicated by equations (54) is valid.

The conditions under which the wall temperature behind a strong shock wave ($M_b^2 >> 1$, $u_w/u_e \rightarrow 6$) remains essentially at its original value will now be determined. Assume c_p is constant, $\sigma = 1$, $\gamma = 1.4$, μ is proportional to T, $T_w \cong T_b$, and $I_N = 1/[(1 + b - c)(N + 1)]$. The latter is the leading term in the expansion for I_N when equations (D3) and (D4) of appendix D are used. The following relations can then be obtained:

3959

CT-4

$$\left.\begin{aligned}
\frac{\theta/\tilde{\delta}}{1 - u_w/u_e} &= \frac{7 + 2(u_w/u_e)}{72} \\
&= \frac{19}{72} \qquad \text{for} \quad u_w/u_e = 6 \\
\frac{T_m}{T_e} &= \frac{5.56(u_w/u_e) - 0.28\left[1 + (u_w/u_e)^2\right]}{6(u_w/u_e) - 1} \\
&\cong \left(\frac{23}{35}\right) \qquad \text{for } (u_w/u_e) = 6 \\
\varphi &= \left(\frac{T_e}{T_m}\right)^{1/2} \\
&\cong \left(\frac{35}{23}\right)^{1/2} \qquad \text{for } (u_w/u_e) = 6
\end{aligned}\right\} \tag{55}$$

Evaluating B for $u_w/u_e = 6$ and substituting into equations (54) yield, for $M_b^2 \gg 1$,

$$\frac{T_w - T_b}{T_b} \cong \frac{0.08}{3} \sqrt{\frac{\alpha_{0-}}{\alpha_e}} \frac{k_e}{k_{0-}} \left(\frac{xu_e}{\nu_e}\right)^{3/10} M_b^2 \tag{56}$$

Assume the fluid to be air and the wall to be cast iron, both initially at $T_b = 530^\circ$ R. It is consistent with the assumptions of $\mu \propto T$, $\sigma = 1$, and so forth, to consider $k_e/\sqrt{\alpha_e} = k_w/\sqrt{\alpha_w}$. Then $\sqrt{\frac{\alpha_{0-}}{\alpha_w}} \frac{k_w}{k_{0-}} = 0.0004$, using the property values of reference 7 for $T_w = T_b = 530^\circ$ R. Equation (56) becomes

$$\frac{T_w - T_b}{T_b} \cong 10^{-5} \left(\frac{xu_e}{\nu_e}\right)^{3/10} M_b^2 \tag{57}$$

Thus, when M_b is large, the wall surface temperature will remain within 10 percent of its original value for $(xu_e/\nu_e)^{3/10} M_b^2 < O(10^4)$.

The preceding solution requires that the wall thickness be at least greater than the wall thermal-boundary-layer thickness (eq. (36)).

CORRELATION OF DATA

In order to correlate the data pertaining to the boundary layer behind a wave, it is necessary to define a Reynolds number which characterizes the flow.

Consider the $t,\bar{x}$-diagram for the flow behind a wave (sketch (a)).

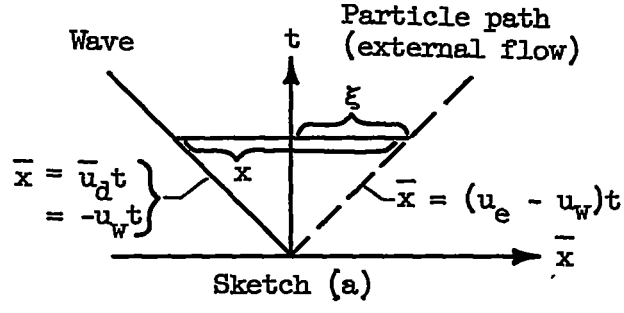

Sketch (a)

An expansion wave is indicated in sketch (a) for convenience. When a particle of the external stream has moved a distance $\xi = (u_e - u_w)t$ relative to the wall, it is a distance $x = \xi + u_w t$, or $x = \xi/(1 - u_w/u_e)$, behind the wave. Thus, $\xi = x(1 - u_w/u_e)$ is a physical dimension (corresponding to a given x) which characterizes the boundary-layer development. Similarly, $(u_w - u_e)$ the velocity of the external flow relative to the wall is the characteristic velocity. The Reynolds number may then be defined as $Re = \xi(u_e - u_w)/\nu_w$ or

$$Re = (u_e x/\nu_w)(1 - u_w/u_e)^2 \tag{58}$$

where ν is arbitrarily referenced to the wall temperature. Equation (58) reduces to $Re = (u_e x/\nu_w)$ for $u_w = 0$. Equation (58) differs by the factor u_e/u_w from the Reynolds number defined by equations (32) of reference 1. For $u_w/u_e = 1$, the Reynolds number of reference 1 agrees with equation (58), but for other values of u_w/u_e, the two Reynolds numbers differ. In particular, the Reynolds number of reference 1 becomes infinite as $u_w \to 0$. Hence, equation (58) appears to be a more useful form.

The correlation of the laminar-boundary-layer skin-friction and heat-transfer data will now be indicated. The local skin-friction coefficient may be defined as

$$c_f = \frac{\tau_w}{\frac{1}{2}\rho_w(u_w - u_e)^2} \tag{59}$$

Therefore, using equations (16a), (58), and (59),

$$c_f\sqrt{Re} = \frac{\sqrt{2}\ f''(0)}{\left|u_w/u_e - 1\right|} \tag{60}$$

where $c_f\sqrt{Re}$ is positive if the wall shear is in the +x-direction. Equation (60) is positive for $0 \leq u_w/u_e < 1$ and negative for $u_w/u_e > 1$. The magnitude of $c_f\sqrt{Re}$ increases monotonically from 0.664 at $u_w/u_e = 0$ to 1.128 at $u_w/u_e = 1$ and 2.291 at $u_w/u_e = 6$. Using equations (16) and (27), the Reynolds analogy can be written as,

3959

CT-4 back

for $0 \leq u_w/u_e \leq 1$,

$$\frac{q_w}{\tau_w}\frac{u_w - u_e}{T_w - T_r}\frac{(\sigma_w)^{0.65-0.15(u_w/u_e)}}{c_{p,w}} = 1 \tag{61a}$$

for $1 \leq u_w/u_e \leq 6$,

$$\frac{q_w}{\tau_w}\frac{u_w - u_e}{T_w - T_r}\frac{(\sigma_w)^{0.52-0.022(u_w/u_e)}}{c_{p,w}} = 1 \tag{61b}$$

The exponent of σ_w is seen to decrease from a value of 0.65 at $u_w/u_e = 0$ to a value of 0.39 at $u_w/u_e = 6$.

By using equation (50a), together with the definitions of Re and c_f as given by equations (58) and (59), the turbulent skin friction can be expressed as

$$c_f Re^{1/5} = 0.0920\left[\left(\frac{T_w}{T_e}\frac{\theta}{\tilde{\delta}}\frac{1}{1 - \frac{u_w}{u_e}}\right)\frac{\nu_m}{\nu_w}\left(\frac{\rho_m}{\rho_w}\right)^4\right]^{1/5}\frac{1 - \frac{u_w}{u_e}}{\left|1 - \frac{u_w}{u_e}\right|} \tag{62}$$

The Reynolds analogy proposed for the turbulent case is given by equation (52), which may be rewritten as

$$\frac{q_w}{\tau_w}\frac{(u_e - u_w)}{(T_w - T_r)}\frac{\sigma_m^{2/3}}{c_{p,m}} = 1 \tag{63}$$

Comparison of equations (61) and (63) suggests (except for the use of a mean reference temperature in eq. (63)) that the exponent of σ_m should decrease with increasing u_w/u_e. However, the use of the exponent 2/3 is probably within the accuracy of the other assumptions involved in the turbulent-boundary-layer analysis.

In reference 4, the boundary layer behind a wave was estimated by using the concept of "an equivalent semi-infinite flat plate." That is, reference 4 assumed "... the properties of a lamina of fluid in the shock tube which has been in motion with a velocity $(u_e - u_w)$ for a time t are equivalent to those of a lamina of fluid which has progressed rearward for a period of time t from the leading edge of a semi-infinite flat plate in a steady flow with free-stream velocity $(u_e - u_w)$...." 3959
For the laminar case, this is equivalent to replacing equation (60) by

$$c_f\sqrt{Re} = 0.664 \frac{1 - u_w/u_e}{\left|1 - u_w/u_e\right|} \tag{64}$$

which is accurate for $u_w/u_e \ll 1$, but underestimates the shear by a factor of 1.7 at $u_w/u_e = 1$ and by a factor of 3.4 at $u_w/u_e = 6$. For the turbulent case, this is equivalent to using equation (62), but with $\frac{\theta}{\delta^*}\Big/\left(1 - \frac{u_w}{u_e}\right)$ evaluated for $u_w/u_e = 0$. If the variation of fluid state properties is neglected, equation (62) can be expressed as

$$c_f Re^{1/5} = 0.0577 \left(1 + \frac{2}{7}\frac{u_w}{u_e}\right)^{1/5} \frac{1 - (u_w/u_e)}{\left|1 - (u_w/u_e)\right|} \tag{65}$$

which has the values 0.0577, 0.0607, and 0.0705 at $u_w/u_e = 0$, 1, and 6, respectively. The fact that the values of $c_f Re^{1/5}$ for $u_w/u_e = 0$ and 1 differ relatively little suggests that the equivalent flat-plate approach may give reasonable estimates for the turbulent boundary layer behind a weak wave. Another interpretation is that (by comparison with the laminar solution) the present method underestimates the wall shear for values of u_w/u_e other than those satisfying $u_w/u_e \ll 1$. Note that the seventh-power velocity profile and the Blasius relation between shear and boundary-layer thickness (eq. (45)) apply to fully developed turbulent pipe flow as well as to the turbulent flow over a semi-infinite flat plate. It is hoped that these expressions are sufficiently universal so that they can be used herein without modification, except to use velocities relative to the wall. The validity of this approach must ultimately be verified by experiment.

CONCLUDING REMARKS

The boundary layer behind a shock or thin expansion wave moving into a stationary fluid has been studied. Both laminar and turbulent boundary layers were considered. The wall temperature behind the waves was also investigated.

For strong shock waves, the boundary layer behind the shock will generally have very large temperature gradients normal to the wall. The assumptions upon which the laminar-boundary-layer solutions were obtained (eqs. (8)) may then have to be reevaluated. It may be possible to obtain more accurate estimates of the laminar boundary layer by using some mean reference temperatures as discussed in appendix C. The choice of the appropriate mean temperature might be obtained from either experimental data or by comparison with more accurate integrations of the laminar-boundary-layer equations.

3959

The turbulent-boundary-layer solutions presented herein represent an extension of empirical, semi-infinite flat-plate, boundary-layer data to the case where the wall is moving. The basic assumptions (especially those incorporated in eqs. (40), (41), and (48)) must ultimately be verified by experiment, particularly for the case of strong shocks.

It should also be noted that the fluid behind a very strong shock may be dissociated. Such dissociation introduces complexities of the boundary-layer problem that are beyond the scope of this report. Experimental studies of the boundary layer behind very strong shocks would yield fundamental information relating to boundary-layer development in a dissociated fluid.

Lewis Flight Propulsion Laboratory
National Advisory Committee for Aeronautics
Cleveland, Ohio, February 16, 1956

APPENDIX A

SYMBOLS

A	function defined by eq. (32b)
a	local speed of sound
B	function defined by eqs. (54)
b	function defined by eqs. (41)
c	function defined by eqs. (41)
c_f	local skin-friction coefficient, $\tau_w \Big/ \frac{1}{2} \rho_w (u_w - u_e)^2$
c_p	specific heat at constant pressure
erfc	complimentary error function
f	function of η defined by eq. (6)
I_N	integral defined by eq. (43) where $N=6,7,$ or 8
k	thermal conductivity
M	Mach number in x,y-coordinate system, $M_e \equiv (u_e/a_e)$, etc.
p	pressure
q	rate of heat transfer in +y-direction
R	gas constant
Re	Reynolds number, $\frac{u_e x}{\nu_w}\left(1 - \frac{u_w}{u_e}\right)^2$
r	function defined by eqs. (15)
s	function defined by eqs. (15)
T	absolute static temperature, $^{\circ}R$
T_m	absolute mean static temperature (e.g., eq. (47)), $^{\circ}R$
T_r	absolute wall surface static temperature for zero heat transfer, $^{\circ}R$
t	time

3959

3959

u,v velocities parallel to x,y-axes

u_w velocity of wall in x,y-coordinate system

$\bar{u},\bar{v}$ velocities parallel to $\bar{x},\bar{y}$-axes

$\bar{u}_d$ velocity of wave in $\bar{x},\bar{y}$-coordinate system

x,y coordinates stationary with respect to wave (fig. 1(b))

$\bar{x},\bar{y}$ coordinates stationary with respect to wall (fig. 1(a))

α diffusivity, $k/\rho c_p$

γ ratio of specific heats

Δ_T wall thermal-boundary-layer thickness corresponding to $\frac{T - T_w}{T_b - T_w} = 0.99$

δ fluid velocity-boundary-layer thickness corresponding to $\frac{u - u_w}{u_e - u_w} = 0.99$

δ_T fluid thermal-boundary-layer thickness corresponding to $\frac{T - T_w}{T_e - T_w} = 0.99$

$\tilde{\delta}$ fluid velocity-boundary-layer thickness from Pohlhausen viewpoint

δ^* fluid boundary-layer displacement thickness, $\int_0^\infty \left(1 - \frac{\rho u}{\rho_e u_e}\right) dy$

ζ similarity parameter for integral solution of laminar case, $\eta/\eta_{\tilde{\delta}}$

ζ_T similarity parameter for integral solution of turbulent case, $y/\tilde{\delta}$

η similarity parameter, eq. (5)

$\eta_{\tilde{\delta}}$ value of η corresponding to $y = \tilde{\delta}$

θ fluid boundary-layer momentum thickness, $\int_0^\infty \frac{\rho u}{\rho_e u_e}\left(1 - \frac{u}{u_e}\right) dy$

μ coefficient of viscosity

ν kinematic viscosity

ρ mass density

σ Prandtl number, $\mu c_p/k$

τ_w local shear stress exerted by fluid on wall

φ function defined by eq. (46b)

ψ stream function (eqs. (4))

Subscripts:

b undisturbed flow ahead of wave

e flow external to fluid boundary layer

m quantity evaluated at T_m

w quantity evaluated just above wall surface, $y = 0^+$

0^- quantity evaluated just below wall surface, $y = 0^-$

Superscripts:

$'$ denotes differentiation with respect to η

Special notation:

$O(\ )$ order of magnitude

3959

3959

CT-5

APPENDIX B

WAVE RELATIONS

For convenience, useful equations relating conditions across a wave are noted herein. Shock waves and expansion waves are considered separately.

Shock wave $(u_w/u_e > 1)$. - Consider the flow in the x,y-coordinate system (i.e., coordinate system moving with the shock). Let subscript b designate the undisturbed flow upstream of the shock wave and

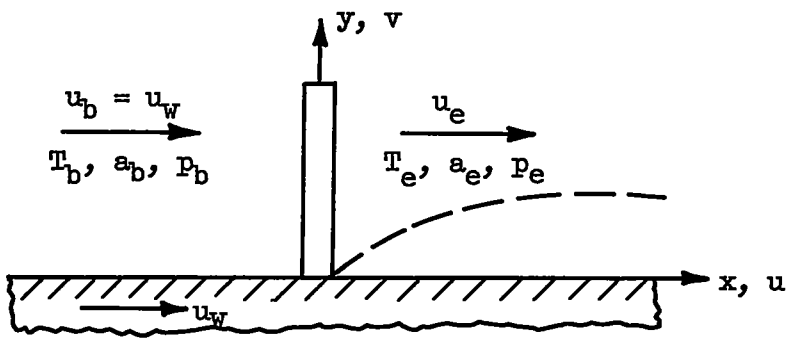

subscript e the flow downstream of the shock wave and external to the boundary layer. Note that $u_b = u_w$ so that $M_b \equiv u_b/a_b = u_w/a_b$. Then, from ordinary shock-wave theory,

$$\left.\begin{aligned} \frac{u_w}{u_e} &= \frac{(\gamma + 1)M_b^2}{(\gamma - 1)M_b^2 + 2} \\ &= \frac{6M_b^2}{M_b^2 + 5} \qquad \text{for } \gamma = 1.4 \end{aligned}\right\} \tag{B1}$$

$$\left.\begin{aligned} M_b^2 &= \frac{2u_w/u_e}{(\gamma + 1) - (\gamma - 1)(u_w/u_e)} \\ &= \frac{5u_w/u_e}{6 - (u_w/u_e)} \qquad \text{for } \gamma = 1.4 \end{aligned}\right\} \tag{B2}$$

$$\left.\begin{aligned} M_e^2 &= \frac{2}{(\gamma + 1)(u_w/u_e) - (\gamma - 1)} \\ &= \frac{5}{6(u_w/u_e) - 1} \qquad \text{for } \gamma = 1.4 \end{aligned}\right\} \tag{B3}$$

$$\left.\begin{aligned} \frac{T_e}{T_b} &= \frac{(\gamma + 1)(u_w/u_e) - (\gamma - 1)}{(u_w/u_e)[(\gamma + 1) - (\gamma - 1)(u_w/u_e)]} \\ &= \frac{6(u_w/u_e) - 1}{(u_w/u_e)\left[6 - (u_w/u_e)\right]} \qquad \text{for } \gamma = 1.4 \end{aligned}\right\} \tag{B4}$$

3959

Expansion wave $(u_w/u_e) < 1)$. - The expansion wave is assumed to have negligible thickness. In the $\bar{x},\bar{y}$-coordinate system (i.e., fixed with respect to wall), the actual and assumed form of the expansion wave is as follows:

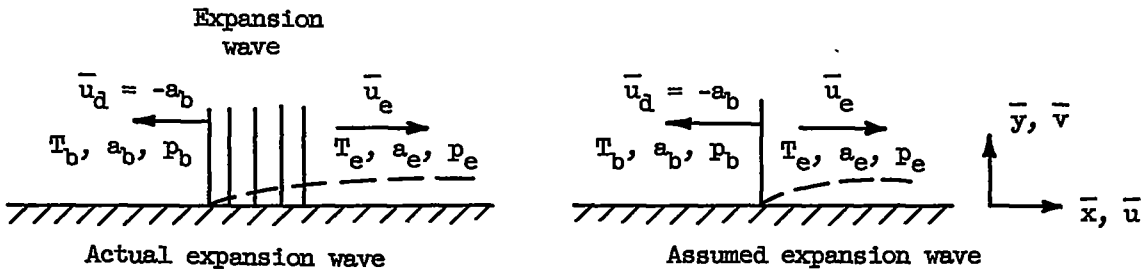

The discontinuity moves with velocity $\bar{u}_d = -a_b$ into the undisturbed fluid. Conditions on either side of the assumed expansion wave are the same as shown for the actual wave. In the x,y-coordinate system the following figure applies:

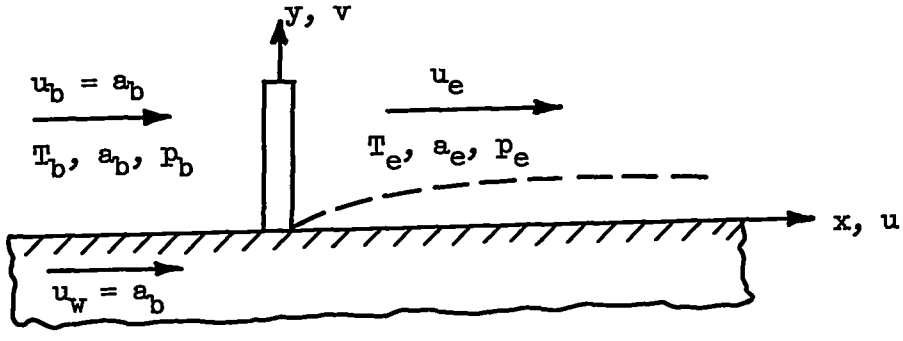

The state properties across the wave are defined by the isentropic relations $a_e/a_b = (T_e/T_b)^{1/2} = (\rho_e/\rho_b)^{\frac{\gamma-1}{2}} = (p_e/p_b)^{\frac{\gamma-1}{2\gamma}}$. Other equations of interest are

$$\left.\begin{aligned} \frac{p_e}{p_b} &= \left[1 - \frac{\gamma - 1}{2}\,\frac{1 - (u_w/u_e)}{u_w/u_e}\right]^{2\gamma/(\gamma-1)} \\ &= \left[\frac{6(u_w/u_e) - 1}{5u_w/u_e}\right]^7 \qquad \text{for } \gamma = 1.4 \end{aligned}\right\} \tag{B5}$$

$$\left.\begin{aligned} \frac{u_w}{u_e} &= \frac{(\gamma - 1)}{(\gamma + 1) - 2(p_e/p_b)^{(\gamma-1)/2\gamma}} \\ &= \frac{1}{6 - 5(p_e/p_b)^{1/7}} \qquad \text{for } \gamma = 1.4 \end{aligned}\right\} \tag{B6}$$

$$\left.\begin{aligned} M_e &= \frac{2}{(\gamma + 1)(u_w/u_e) - (\gamma - 1)} \\ &= \frac{5}{6(u_w/u_e) - 1} \qquad \text{for } \gamma = 1.4 \end{aligned}\right\} \tag{B7}$$

$$\left.\begin{aligned} \frac{T_e}{T_b} &= \left[1 - \frac{\gamma - 1}{2}\,\frac{1 - (u_w/u_e)}{u_w/u_e}\right]^2 \\ &= \left[\frac{6(u_w/u_e) - 1}{5u_w/u_e}\right]^2 \qquad \text{for } \gamma = 1.4 \end{aligned}\right\} \tag{B8}$$

3959

CT-5 back

APPENDIX C

LAMINAR-BOUNDARY-LAYER SOLUTION REFERENCED TO A MEAN TEMPERATURE

In the body of this report, the laminar-boundary-layer solution was obtained by assuming that μ and k are proportional to T and that σ and c_p are constant, all referenced to wall conditions (eqs. (8)). The question naturally arises as to whether the use of a mean reference temperature T_m would lead to more accurate correlations with exact (in regard to fluid properties) integrations of the laminar-boundary-layer equations. 3956

If a mean reference temperature is used in equations (16), they become

$$\tau_w = u_e f''(0)\sqrt{\frac{u_e \rho_m \mu_m}{2x}} \tag{C1}$$

$$q_w = -s'(0)(T_w - T_r)\sqrt{\frac{u_e \rho_m \mu_m}{2x}}\left(\frac{c_{p,m}}{\sigma_m}\right) \tag{C2}$$

$$\frac{v_e}{u_e} = \frac{\rho_m}{\rho_e}\sqrt{\frac{\nu_m}{2xu_e}}\left[\lim_{\eta\to\infty}(\eta - f) + \left(\frac{u_w}{u_e} - 1\right)^2 \frac{u_e^2}{2T_e c_{p,m}}\int_0^\infty r\,d\eta + \left(\frac{T_w}{T_e} - \frac{T_r}{T_e}\right)\int_0^\infty s\,d\eta\right] \tag{C3}$$

where

$$\frac{T_r}{T_e} = 1 + \left(\frac{u_w}{u_e} - 1\right)^2 \frac{u_e^2 r(0)}{2T_e c_{p,m}} \tag{C4}$$

and the solutions for r and s are considered functions of σ_m. In reference 13, it is found that the choice

$$T_m = 0.5(T_w + T_e) + 0.22(T_r - T_e) \tag{C5}$$

correlated equations (C1) and (C2) with accurate integrations of the boundary-layer equations. Flow past a semi-infinite flat plate is considered therein. Equation (C5) should also provide improved estimates for τ_w and q_w for $u_w/u_e \neq 0$. If v_e/u_e is to be correlated with accurate integrations of the boundary-layer equations, another estimate for T_m might be called for. Note that equation (C5) defines the mean temperature which was used in the turbulent-boundary-layer analysis.

3959

APPENDIX D

EVALUATION OF I_N

The turbulent-boundary-layer analysis requires evaluation of the integral

$$I_N = \int_0^1 \frac{z^N dz}{1 + bz - cz^2} \tag{43}$$

3959

where $N = 6, 7,$ or 8, and

$$b = \frac{T_r}{T_w} - 1$$

$$c = \left(\frac{T_r}{T_e} - 1\right)\frac{T_e}{T_w}$$

The denominator of equation (43) may be factored so that $(-c)(x - \lambda)(x - \beta) \equiv 1 + bx - cx^2$ where

$$\lambda = \frac{1}{2c}\left(b + \sqrt{b^2 + 4c}\right)$$

$$\beta = \frac{1}{2c}\left(b - \sqrt{b^2 + 4c}\right)$$

from physical arguments $b > -1$, $c \geq 0$, and $0 \leq \frac{c}{1 + b} < 1$. It can then be shown that $\beta < 0$ and $\lambda > 1$. Equation (43) can now be written as

$$I_N = \frac{1}{\sqrt{b^2 + 4c}}\left(I_{N,\beta} - I_{N,\lambda}\right) \tag{D1}$$

where

$$I_{N,\beta} \equiv \int_0^1 \frac{z^N dz}{z - \beta}$$

$$I_{N,\lambda} \equiv \int_0^1 \frac{z^N dz}{z - \lambda}$$

3959

The integrals $I_{N,\beta}$ and $I_{N,\lambda}$ can be integrated as follows:

$$I_{N,\beta} = \int_0^1 \frac{z^N dz}{z - \beta} = \beta^N \int_0^1 \frac{dz}{z - \beta} + \int_0^1 \left(\frac{z^N - \beta^N}{z - \beta}\right) dz$$

$$= \beta^N \left[\ln\left(\frac{\beta - 1}{\beta}\right) + \sum_{m=1}^{N} \frac{1}{m}\left(\frac{1}{\beta}\right)^m\right] \tag{D2a}$$

Similarly, for $I_{N,\lambda}$,

$$I_{N,\lambda} = \lambda^N \left[\ln\left(\frac{\lambda - 1}{\lambda}\right) + \sum_{m=1}^{N} \frac{1}{m}\left(\frac{1}{\lambda}\right)^m\right] \tag{D2b}$$

The logarithm term is very nearly equal and opposite to the summation term, in equations (D2a) and (D2b), for values of β not close to zero and values of λ not close to 1, respectively. Hence, each of these terms must be evaluated very accurately in order to get accurate estimates of $I_{N,\beta}$ and $I_{N,\lambda}$. For values of β not close to zero and values of λ not close to 1, alternate expressions for $I_{N,\beta}$ and $I_{N,\lambda}$ are desirable. Since $\beta < 0$,

$$I_{N,\beta} = \frac{1}{1 - \beta} \int_0^1 \frac{z^N dz}{1 - \left(\frac{1 - z}{1 - \beta}\right)} = \frac{1}{1 - \beta} \sum_{m=0}^{\infty} \int_0^1 z^N \left(\frac{1 - z}{1 - \beta}\right)^m dz$$

$$= \frac{1}{1 - \beta} \sum_{m=0}^{\infty} \frac{N!m!}{(N + m + 1)!} \left(\frac{1}{1 - \beta}\right)^m$$

$$= \frac{1}{(N + 1)(1 - \beta)} \left[1 + \frac{1!}{(N + 2)(1 - \beta)} + \frac{2!}{(N + 3)(N + 2)(1 - \beta)^2} + \cdots\right] \tag{D3}$$

Since $\lambda > 1$,

$$I_{N,\lambda} = \int_0^1 \frac{z^N dz}{1 - \lambda} - \frac{1}{\lambda(1 - \lambda)} \sum_{m=0}^{\infty} \left(\int_0^1 (1 - z) z^N \left(\frac{z}{\lambda}\right)^m dz \right)$$

$$= \frac{1}{(N + 1)(1 - \lambda)} \left[1 - (N + 1) \sum_{m=1}^{\infty} \frac{1}{(N + m)(N + m + 1)} \left(\frac{1}{\lambda}\right)^m \right]$$

$$= \frac{1}{(N + 1)(1 - \lambda)} \left[1 - \frac{(N + 1)}{(N + 1)(N + 2)\lambda} - \frac{(N + 1)}{(N + 2)(N + 3)\lambda^2} - \ldots \right] \tag{D4}$$

Equations (D3) and (D4) converge rapidly for $\beta \ll 0$ and $\lambda \gg 1$.

REFERENCES

1. Mirels, Harold: Laminar Boundary Layer Behind Shock Advancing into Stationary Fluid. NACA TN 3401, 1955.

2. Donaldson, Coleman duP., and Sullivan, Roger D.: The Effect of Wall Friction on the Strength of Shock Waves in Tubes and Hydraulic Jumps in Channels. NACA TN 1942, 1949.

3. Hollyer, Robert N., Jr.: A Study of Attenuation in the Shock Tube. Eng. Res. Inst., Univ. of Michigan, July 1, 1953. (U.S. Navy Dept., Office Naval Res. Contract No. N6-ONR-232-TO IV, Proj. M720-4.)

4. Trimpi, Robert L., and Cohen, Nathaniel B.: A Theory for Predicting the Flow of Real Gases in Shock Tubes with Experimental Verification. NACA TN 3375, 1955.

5. Chapman, Dean R., and Rubesin, Morris W.: Temperature and Velocity Profiles in the Compressible Laminar Boundary Layer with Arbitrary Distribution of Surface Temperature. Jour. Aero. Sci., vol. 16, no. 9, Sept. 1949, pp. 547-565.

6. Low, George M.: The Compressible Laminar Boundary Layer with Heat Transfer and Small Pressure Gradient. NACA TN 3028, 1953.

7. Hartunian, Richard A.: Some Viscous Effects in Shock-Tube Flow. M. S. Thesis, Cornell Univ., June 1954.

8. Rott, N., and Hartunian, R.: On the Heat Transfer to the Walls of a Shock Tube. Graduate School of Aero. Eng., Cornell Univ., Nov. 1955. (Contract AF 33(038)-21406.)

9. Eckert, E. R. G.: Introduction to the Transfer of Heat and Mass. McGraw-Hill Book Co., Inc., 1950, pp. 266-275.

10. Tucker, Maurice: Approximate Calculation of Turbulent Boundary-Layer Development in Compressible Flow. NACA TN 2337, 1951.

11. Bartz, D. R.: An Approximate Solution of Compressible Turbulent Boundary-Layer Development and Convective Heat Transfer in Convergent-Divergent Nozzles. Trans. A.S.M.E., vol. 77, no. 8, Nov. 1955, pp. 1235-1245.

12. Schlichting, H.: Lecture Series "Boundary Layer Theory." Pt. II - Turbulent Flows. NACA TM 1218, 1949.

13. Eckert, Ernst R. G.: Survey on Heat Transfer at High Speeds. Tech. Rep. 54-70, Aero. Res. Lab., Wright Air Dev. Center, Wright-Patterson Air Force Base, Apr. 1954.

3959

CT-6

3959

TABLE I. - LAMINAR BOUNDARY LAYER BEHIND WAVE (EQS. 9 AND 15)

(a) Solution for $u_w/u_e = 0$

η	f	f'	f''	Prandtl number σ_w, 0.72					
				$\int_0^\eta r\,d\eta$	r	$-r'$	$\int_0^\eta s\,d\eta$	s	$-s'$
0.0	0.0000	0.0000	0.4696	0.0000	0.8477	0.0000	0.0000	1.0000	0.4181
.1	.0023	.0470	.4696	.0847	.8461	.0318	.0979	.9582	.4181
.2	.0094	.0939	.4693	.1691	.8414	.0635	.1916	.9164	.4179
.3	.0211	.1408	.4686	.2529	.8334	.0951	.2812	.8746	.4175
.4	.0375	.1876	.4673	.3357	.8224	.1264	.3666	.8329	.4166
.5	.0586	.2342	.4650	.4173	.8082	.1572	.4478	.7913	.4152
.6	.0844	.2806	.4617	.4972	.7909	.1878	.5248	.7499	.4130
.7	.1147	.3265	.4572	.5753	.7708	.2162	.5978	.7087	.4101
.8	.1497	.3720	.4512	.6513	.7478	.2437	.6666	.6679	.4062
.9	.1891	.4167	.4436	.7248	.7221	.2694	.7314	.6275	.4013
1.0	.2330	.4606	.4344	.7956	.6939	.2929	.7921	.5877	.3953
1.1	.2812	.5035	.4234	.8635	.6636	.3138	.8489	.5485	.3880
1.2	.3337	.5452	.4106	.9283	.6313	.3317	.9018	.5101	.3795
1.3	.3902	.5856	.3960	.9897	.5974	.3463	.9510	.4727	.3698
1.4	.4507	.6244	.3797	1.0477	.5621	.3573	.9964	.4362	.3588
1.5	.5150	.6615	.3618	1.1021	.5260	.3646	1.0383	.4009	.3465
1.6	.5830	.6967	.3425	1.1529	.4894	.3680	1.0766	.3669	.3331
1.7	.6543	.7299	.3220	1.2000	.4525	.3675	1.1117	.3344	.3186
1.8	.7289	.7611	.3004	1.2434	.4160	.3633	1.1436	.3033	.3031
1.9	.8064	.7900	.2783	1.2832	.3800	.3555	1.1724	.2738	.2868
2.0	.8868	.8167	.2557	1.3194	.3450	.3444	1.1984	.2459	.2699
2.1	.9697	.8411	.2330	1.3522	.3112	.3305	1.2216	.2198	.2524
2.2	1.0549	.8633	.2106	1.3817	.2790	.3141	1.2424	.1954	.2347
2.3	1.1423	.8833	.1887	1.4081	.2485	.2957	1.2608	.1729	.2168
2.4	1.2315	.9011	.1676	1.4315	.2199	.2758	1.2770	.1521	.1991
2.5	1.3224	.9168	.1475	1.4521	.1933	.2550	1.2913	.1330	.1816
2.6	1.4148	.9306	.1286	1.4702	.1689	.2337	1.3037	.1157	.1646
2.7	1.5085	.9426	.1111	1.4860	.1466	.2122	1.3145	.1001	.1481
2.8	1.6033	.9529	.0951	1.4996	.1264	.1918	1.3238	.0861	.1324
2.9	1.6990	.9616	.0806	1.5114	.1083	.1709	1.3317	.0736	.1176
3.0	1.7956	.9691	.0677	1.5214	.0922	.1514	1.3385	.0625	.1037
3.1	1.8928	.9752	.0563	1.5299	.0780	.1331	1.3443	.0528	.0908
3.2	1.9906	.9804	.0464	1.5370	.0656	.1161	1.3491	.0443	.0789
3.3	2.0888	.9846	.0378	1.5430	.0548	.1005	1.3532	.0370	.0682
3.4	2.1875	.9880	.0305	1.5480	.0454	.0863	1.3566	.0307	.0584
3.5	2.2864	.9907	.0244	1.5522	.0375	.0735	1.3594	.0253	.0497
3.6	2.3856	.9929	.0193	1.5556	.0307	.0628	1.3617	.0207	.0420
3.7	2.4850	.9946	.0152	1.5583	.0250	.0533	1.3635	.0168	.0353
3.8	2.5845	.9958	.0118	1.5606	.0202	.0436	1.3650	.0136	.0294
3.9	2.6841	.9970	.0090	1.5624	.0162	.0360	1.3663	.0109	.0243
4.0	2.7839	.9978	.0069	1.5639	.0129	.0296	1.3673	.0087	.0120
4.1	2.8837	.9984	.0052	1.5650	.0103	.0242	1.3680	.0069	.0163
4.2	2.9835	.9988	.0039	1.5659	.0081	.0196	1.3686	.0055	.0132
4.3	3.0834	.9992	.0029	1.5666	.0063	.0157	1.3691	.0043	.0106
4.4	3.1834	.9994	.0021	1.5672	.0049	.0125	1.3695	.0033	.0085
4.5	3.2833	.9996	.0015	1.5676	.0038	.0099	1.3698	.0023	.0067
4.6	3.3833	.9997	.0011	1.5680	.0029	.0078	1.3700	.0020	.0053
4.7	3.4833	.9998	.0008	1.5682	.0022	.0061	1.3702	.0015	.0041
4.8	3.5832	.9999	.0005	1.5684	.0017	.0047	1.3703	.0011	.0032
4.9	3.6832	.9999	.0004	1.5686	.0013	.0036	1.3704	.0009	.0025
5.0	3.7832	.9999	.0003	1.5687	.0009	.0028	1.3705	.0006	.0019
5.1	3.8832	1.0000	.0002	1.5688	.0007	.0021	1.3706	.0005	.0014
5.2	3.9832	1.0000	.0001	1.5688	.0005	.0016	1.3706	.0003	.0011
5.3	4.0832	1.0000	.0001	1.5689	.0004	.0012	1.3706	.0003	.0008
5.4	4.1832	1.0000	.0001	1.5689	.0003	.0009	1.3706	.0002	.0006
5.5	4.2832	1.0000	.0000	1.5689	.0002	.0007	1.3707	.0001	.0004
5.6	4.3832	1.0000	.0000	1.5689	.0001	.0005	1.3707	.0001	.0003
5.7	4.4832	1.0000	.0000	1.5690	.0001	.0003	1.3707	.0001	.0002
5.8	4.5832	1.0000	.0000	1.5690	.0001	.0003	1.3707	.0000	.0002
5.9	4.6832	1.0000	.0000	1.5690	.0001	.0002	1.3707	.0000	.0001
6.0	4.7832	1.0000	.0000	1.5690	.0000	.0001	1.3707	.0000	.0001
6.1	4.8832	1.0000	.0000	1.5690	.0000	.0001	1.3707	.0000	.0001
6.2	4.9832	1.0000	.0000	1.5690	.0000	.0001	1.3707	.0000	.0000
6.3	5.0832	1.0000	.0000	1.5690	.0000	.0000	1.3707	.0000	.0000

CT-6 back 3959

TABLE I. - Continued. LAMINAR BOUNDARY LAYER BEHIND WAVE (EQS. 9 AND 15)

(b) Solution for $u_w/u_e = 0.25$

η	f	f'	f''	Prandtl number σ_w, 0.72					
				$\int_0^\eta r\,d\eta$	r	$-r'$	$\int_0^\eta s\,d\eta$	s	$-s'$
0.0	0.0000	0.2500	0.4295	0.0000	0.8628	0.0000	0.0000	1.0000	0.4996
.1	.0271	.2929	.4290	.0868	.8604	.0473	.0975	.9501	.4992
.2	.0546	.3358	.4272	.1719	.8534	.0939	.1900	.9002	.4976
.3	.0943	.3783	.4239	.2567	.8417	.1396	.2776	.8506	.4949
.4	.1342	.4205	.4191	.3401	.8255	.1838	.3601	.8013	.4909
.5	.1784	.4621	.4126	.4217	.8050	.2258	.4378	.7524	.4854
.6	.2266	.5029	.4044	.5010	.7804	.2649	.5106	.7042	.4784
.7	.2789	.5429	.3943	.5776	.7521	.3006	.5787	.6568	.4698
.8	.3352	.5817	.3824	.6513	.7203	.3323	.6420	.6103	.4595
.9	.3952	.6193	.3687	.7216	.6858	.3593	.7008	.5650	.4476
1.0	.4590	.6554	.3533	.7884	.6488	.3813	.7551	.5209	.4340
1.1	.5263	.6899	.3363	.8513	.6098	.3979	.8050	.4782	.4189
1.2	.5969	.7226	.3179	.9103	.5694	.4090	.8508	.4371	.4023
1.3	.6707	.7535	.2984	.9652	.5281	.4145	.8925	.3978	.3844
1.4	.7475	.7823	.2780	1.0159	.4866	.4146	.9304	.3603	.3653
1.5	.8271	.8090	.2570	1.0625	.4454	.4096	.9646	.3248	.3451
1.6	.9093	.8337	.2356	1.1050	.4049	.3998	.9954	.2913	.3242
1.7	.9938	.8562	.2142	1.1435	.3656	.3859	1.0230	.2600	.3028
1.8	1.0804	.8765	.1931	1.1782	.3278	.3683	1.0475	.2308	.2810
1.9	1.1690	.8948	.1726	1.2092	.2920	.3479	1.0692	.2038	.2591
2.0	1.2593	.9111	.1528	1.2367	.2583	.3252	1.0883	.1789	.2374
2.1	1.3512	.9254	.1341	1.2609	.2270	.3011	1.1051	.1563	.2161
2.2	1.4444	.9379	.1166	1.2821	.1981	.2761	1.1196	.1357	.1955
2.3	1.5387	.9488	.1005	1.3006	.1718	.2508	1.1323	.1171	.1756
2.4	1.6341	.9581	.0857	1.3166	.1480	.2258	1.1431	.1005	.1566
2.5	1.7303	.9660	.0725	1.3303	.1266	.2016	1.1524	.0858	.1387
2.6	1.8272	.9726	.0607	1.3420	.1076	.1784	1.1603	.0728	.1221
2.7	1.9248	.9782	.0503	1.3519	.0909	.1566	1.1670	.0613	.1066
2.8	2.0228	.9827	.0413	1.3602	.0762	.1363	1.1727	.0514	.0925
2.9	2.1213	.9865	.0336	1.3672	.0635	.1178	1.1773	.0428	.0797
3.0	2.2201	.9895	.0270	1.3730	.0526	.1010	1.1812	.0354	.0682
3.1	2.3192	.9919	.0215	1.3778	.0433	.0859	1.1845	.0291	.0579
3.2	2.4184	.9938	.0170	1.3817	.0354	.0725	1.1871	.0238	.0488
3.3	2.5179	.9953	.0133	1.3849	.0287	.0607	1.1892	.0193	.0409
3.4	2.6175	.9965	.0103	1.3875	.0232	.0505	1.1910	.0156	.0340
3.5	2.7172	.9974	.0079	1.3896	.0186	.0417	1.1924	.0125	.0280
3.6	2.8170	.9981	.0060	1.3912	.0148	.0342	1.1935	.0099	.0230
3.7	2.9168	.9986	.0045	1.3925	.0117	.0278	1.1944	.0079	.0187
3.8	3.0167	.9990	.0033	1.3936	.0092	.0225	1.1951	.0062	.0151
3.9	3.1166	.9993	.0024	1.3944	.0072	.0180	1.1956	.0048	.0121
4.0	3.2165	.9995	.0018	1.3950	.0056	.0143	1.1961	.0037	.0096
4.1	3.3165	.9996	.0013	1.3955	.0043	.0113	1.1964	.0029	.0076
4.2	3.4165	.9997	.0009	1.3959	.0033	.0089	1.1966	.0022	.0060
4.3	3.5164	.9998	.0006	1.3962	.0025	.0069	1.1968	.0017	.0047
4.4	3.6164	.9999	.0005	1.3964	.0019	.0054	1.1970	.0013	.0036
4.5	3.7164	.9999	.0003	1.3966	.0014	.0041	1.1971	.0010	.0028
4.6	3.8164	.9999	.0002	1.3967	.0011	.0031	1.1972	.0007	.0021
4.7	3.9164	1.0000	.0001	1.3968	.0008	.0024	1.1972	.0005	.0016
4.8	4.0164	1.0000	.0001	1.3969	.0006	.0018	1.1973	.0004	.0012
4.9	4.1164	1.0000	.0001	1.3969	.0004	.0013	1.1973	.0003	.0009
5.0	4.2164	1.0000	.0000	1.3969	.0003	.0010	1.1973	.0002	.0007
5.1	4.3164	1.0000	.0000	1.3970	.0002	.0007	1.1974	.0001	.0005
5.2	4.4164	1.0000	.0000	1.3970	.0002	.0005	1.1974	.0001	.0003
5.3	4.5164	1.0000	.0000	1.3970	.0001	.0004	1.1974	.0001	.0002
5.4	4.6164	1.0000	.0000	1.3970	.0001	.0003	1.1974	.0001	.0001
5.5	4.7164	1.0000	.0000	1.3970	.0001	.0002	1.1974	.0000	.0001
5.6	4.8164	1.0000	.0000	1.3970	.0000	.0001	1.1974	.0000	.0001
5.7	4.9164	1.0000	.0000	1.3970	.0000	.0001	1.1974	.0000	.0001
5.8	5.0164	1.0000	.0000	1.3970	.0000	.0001	1.1974	.0000	.0000
5.9	5.1164	1.0000	.0000	1.3970	.0000	.0000	1.1974	.0000	.0000

3959

TABLE I. - Continued. LAMINAR BOUNDARY LAYER BEHIND WAVE (EQS. 9 AND 15)

(c) Solution for $u_w/u_e = 0.50$

η	f	f'	f''	Prandtl number σ_w, 0.72					
				$\int_0^\eta r\,d\eta$	r	$-r'$	$\int_0^\eta s\,d\eta$	s	$-s'$
0.0	0.0000	0.5000	0.3287	0.0000	0.8727	0.0000	0.0000	1.0000	0.5665
.1	.0516	.5328	.3279	.0872	.8696	.0621	.0972	.9434	.5654
.2	.1066	.5658	.3253	.1746	.8640	.1230	.1887	.8870	.5628
.3	.1647	.5979	.3210	.2590	.8451	.1817	.2746	.8310	.5568
.4	.2261	.6297	.3147	.3425	.8241	.2370	.3549	.7757	.5490
.5	.2906	.6607	.3067	.4237	.7978	.2878	.4298	.7213	.5389
.6	.3582	.6909	.2969	.5019	.7667	.3330	.4992	.6680	.5265
.7	.4288	.7201	.2855	.5769	.7314	.3719	.5634	.6161	.5118
.8	.5022	.7480	.2725	.6481	.6926	.4038	.6225	.5657	.4949
.9	.5783	.7745	.2582	.7153	.6509	.4282	.6766	.5172	.4760
1.0	.6571	.7996	.2427	.7782	.6072	.4449	.7260	.4706	.4553
1.1	.7382	.8230	.2264	.8367	.5622	.4540	.7708	.4268	.4330
1.2	.8216	.8448	.2094	.8907	.5167	.4558	.8113	.3840	.4094
1.3	.9071	.8649	.1921	.9401	.4713	.4508	.8477	.3443	.3847
1.4	.9945	.8833	.1746	.9849	.4267	.4397	.8802	.3071	.3592
1.5	1.0837	.8999	.1574	1.0254	.3835	.4233	.9092	.2725	.3333
1.6	1.1745	.9147	.1406	1.0617	.3422	.4025	.9348	.2404	.3073
1.7	1.2666	.9280	.1244	1.0940	.3031	.3783	.9574	.2110	.2815
1.8	1.3600	.9397	.1091	1.1224	.2666	.3516	.9771	.1841	.2561
1.9	1.4545	.9499	.0948	1.1474	.2328	.3234	.9943	.1598	.2314
2.0	1.5499	.9587	.0816	1.1691	.2019	.2945	1.0091	.1378	.2077
2.1	1.6462	.9662	.0695	1.1879	.1739	.2656	1.0219	.1182	.1851
2.2	1.7431	.9726	.0587	1.2040	.1488	.2373	1.0328	.1008	.1638
2.3	1.8407	.9780	.0491	1.2177	.1264	.2101	1.0421	.0854	.1440
2.4	1.9387	.9825	.0406	1.2293	.1067	.1845	1.0500	.0719	.1287
2.5	2.0371	.9861	.0333	1.2391	.0895	.1606	1.0566	.0602	.1089
2.6	2.1359	.9892	.0270	1.2473	.0745	.1387	1.0621	.0501	.0937
2.7	2.2349	.9916	.0217	1.2541	.0617	.1188	1.0666	.0414	.0801
2.8	2.3342	.9935	.0173	1.2597	.0507	.1010	1.0704	.0340	.0679
2.9	2.4336	.9951	.0136	1.2643	.0414	.0852	1.0735	.0277	.0572
3.0	2.5332	.9963	.0106	1.2680	.0336	.0713	1.0760	.0225	.0479
3.1	2.6329	.9972	.0082	1.2711	.0271	.0593	1.0780	.0181	.0397
3.2	2.7326	.9979	.0063	1.2735	.0217	.0489	1.0796	.0145	.0328
3.3	2.8325	.9985	.0048	1.2754	.0173	.0400	1.0809	.0116	.0268
3.4	2.9323	.9989	.0036	1.2770	.0137	.0325	1.0820	.0091	.0218
3.5	3.0322	.9992	.0026	1.2782	.0107	.0262	1.0828	.0072	.0176
3.6	3.1322	.9994	.0019	1.2791	.0084	.0210	1.0834	.0056	.0141
3.7	3.2321	.9996	.0014	1.2799	.0065	.0167	1.0839	.0043	.0112
3.8	3.3321	.9997	.0010	1.2805	.0050	.0132	1.0843	.0033	.0088
3.9	3.4321	.9998	.0007	1.2809	.0038	.0104	1.0846	.0025	.0069
4.0	3.5321	.9999	.0005	1.2812	.0029	.0081	1.0848	.0019	.0054
4.1	3.6320	.9999	.0004	1.2815	.0022	.0062	1.0850	.0015	.0042
4.2	3.7320	.9999	.0002	1.2817	.0016	.0048	1.0851	.0011	.0032
4.3	3.8320	1.0000	.0002	1.2818	.0012	.0036	1.0852	.0008	.0024
4.4	3.9320	1.0000	.0001	1.2819	.0009	.0028	1.0853	.0006	.0018
4.5	4.0320	1.0000	.0001	1.2820	.0007	.0021	1.0853	.0004	.0014
4.6	4.1320	1.0000	.0001	1.2821	.0005	.0015	1.0853	.0003	.0010
4.7	4.2320	1.0000	.0000	1.2821	.0004	.0011	1.0854	.0002	.0008
4.8	4.3320	1.0000	.0000	1.2821	.0003	.0008	1.0854	.0002	.0006
4.9	4.4320	1.0000	.0000	1.2822	.0002	.0006	1.0854	.0001	.0004
5.0	4.5320	1.0000	.0000	1.2822	.0001	.0004	1.0854	.0001	.0003
5.1	4.6320	1.0000	.0000	1.2822	.0001	.0003	1.0854	.0001	.0002
5.2	4.7320	1.0000	.0000	1.2822	.0001	.0002	1.0854	.0000	.0002
5.3	4.8320	1.0000	.0000	1.2822	.0001	.0002	1.0854	.0000	.0001
5.4	4.9320	1.0000	.0000	1.2822	.0000	.0001	1.0854	.0000	.0001
5.5	5.0320	1.0000	.0000	1.2822	.0000	.0001	1.0854	.0000	.0001
5.6	5.1320	1.0000	.0000	1.2822	.0000	.0001	1.0854	.0000	.0000
5.7	5.2320	1.0000	.0000	1.2822	.0000	.0000	1.0854	.0000	.0000
5.8	5.3320	1.0000	.0000	1.2822	.0000	.0000	1.0854	.0000	.0000
5.9	5.4320	1.0000	.0000	1.2822	.0000	.0000	1.0854	.0000	.0000
6.0	5.5320	1.0000	.0000	1.2822	.0000	.0001	1.0854	.0000	.0000
6.1	5.6320	1.0000	.0000	1.2822	.0000	.0000	1.0854	.0000	.0000

3959

TABLE I. - Continued. LAMINAR BOUNDARY LAYER BEHIND WAVE (EQS. 9 AND 15)

(d) Solution for $u_w/u_e = 0.75$

η	f	f'	f''	Prandtl number σ_w, 0.72					
				$\int_0^\eta r\,d\eta$	r	$-r'$	$\int_0^\eta s\,d\eta$	s	$-s'$
0.0	0.0000	0.7500	0.1828	0.0000	0.8729	0.0000	0.0000	1.0000	0.6847
.1	.0759	0.7683	.1822	.0879	.8761	.0767	.0989	.9376	.6230
.2	.1536	0.7864	.1801	.1750	.8647	.1514	.1875	.8755	.6179
.3	.2332	0.8042	.1766	.2606	.8460	.2221	.2720	.8141	.6093
.4	.3145	0.8217	.1719	.3439	.8204	.2871	.3504	.7538	.5974
.5	.3975	0.8386	.1659	.4244	.7888	.3448	.4228	.6948	.5823
.6	.4822	0.8548	.1587	.5015	.7518	.3938	.4894	.6374	.5648
.7	.5684	0.8703	.1506	.5746	.7103	.4333	.5503	.5820	.5432
.8	.6562	0.8849	.1417	.6435	.6654	.4628	.6059	.5288	.5198
.9	.7454	0.8986	.1321	.7077	.6181	.4821	.6562	.4781	.4942
1.0	.8359	0.9113	.1220	.7670	.5694	.4916	.7016	.4300	.4669
1.1	.9276	0.9230	.1117	.8215	.5201	.4918	.7423	.3848	.4382
1.2	1.0204	0.9336	.1014	.8711	.4713	.4838	.7786	.3424	.4085
1.3	1.1143	0.9433	.0911	.9158	.4236	.4685	.8109	.3031	.3783
1.4	1.2091	0.9519	.0811	.9559	.3778	.4473	.8394	.2668	.3479
1.5	1.3046	0.9595	.0715	.9914	.3343	.4214	.8643	.2335	.3178
1.6	1.4009	0.9662	.0625	1.0228	.2936	.3921	.8862	.2032	.2883
1.7	1.4979	0.9720	.0541	1.0503	.2560	.3606	.9051	.1758	.2598
1.8	1.5953	0.9770	.0463	1.0741	.2215	.3281	.9214	.1512	.2324
1.9	1.6932	0.9813	.0393	1.0947	.1903	.2954	.9354	.1293	.2064
2.0	1.7915	0.9849	.0330	1.1123	.1624	.2634	.9474	.1099	.1821
2.1	1.8902	0.9879	.0275	1.1273	.1376	.2327	.9575	.0928	.1595
2.2	1.9891	0.9904	.0226	1.1399	.1158	.2037	.9660	.0779	.1387
2.3	2.0883	0.9925	.0184	1.1505	.0968	.1768	.9731	.0650	.1198
2.4	2.1876	0.9941	.0149	1.1593	.0804	.1521	.9790	.0539	.1027
2.5	2.2871	0.9955	.0119	1.1667	.0663	.1299	.9839	.0444	.0874
2.6	2.3867	0.9965	.0094	1.1727	.0543	.1100	.9880	.0364	.0739
2.7	2.4864	0.9974	.0074	1.1776	.0442	.0925	.9913	.0296	.0620
2.8	2.5862	0.9980	.0057	1.1816	.0358	.0771	.9939	.0239	.0516
2.9	2.6860	0.9985	.0044	1.1848	.0287	.0638	.9961	.0192	.0427
3.0	2.7859	0.9989	.0034	1.1874	.0229	.0525	.9978	.0153	.0351
3.1	2.8858	0.9992	.0025	1.1894	.0182	.0428	.9992	.0121	.0286
3.2	2.9857	0.9994	.0019	1.1910	.0143	.0346	1.0002	.0096	.0231
3.3	3.0856	0.9996	.0014	1.1923	.0112	.0278	1.0011	.0075	.0186
3.4	3.1856	0.9997	.0010	1.1933	.0087	.0222	1.0018	.0058	.0148
3.5	3.2856	0.9998	.0007	1.1941	.0067	.0176	1.0023	.0045	.0118
3.6	3.3856	0.9999	.0005	1.1946	.0052	.0138	1.0027	.0034	.0092
3.7	3.4856	0.9999	.0004	1.1951	.0039	.0108	1.0030	.0026	.0072
3.8	3.5855	0.9999	.0003	1.1954	.0030	.0084	1.0032	.0020	.0056
3.9	3.6855	1.0000	.0002	1.1957	.0022	.0065	1.0034	.0015	.0043
4.0	3.7855	1.0000	.0001	1.1959	.0017	.0049	1.0035	.0011	.0033
4.1	3.8855	1.0000	.0001	1.1960	.0012	.0037	1.0036	.0008	.0025
4.2	3.9855	1.0000	.0001	1.1961	.0009	.0028	1.0037	.0006	.0019
4.3	4.0855	1.0000	.0000	1.1962	.0007	.0021	1.0037	.0004	.0014
4.4	4.1855	1.0000	.0000	1.1963	.0005	.0016	1.0038	.0003	.0010
4.5	4.2855	1.0000	.0000	1.1963	.0004	.0012	1.0038	.0002	.0008
4.6	4.3855	1.0000	.0000	1.1964	.0003	.0008	1.0038	.0002	.0006
4.7	4.4855	1.0000	.0000	1.1964	.0002	.0006	1.0038	.0001	.0004
4.8	4.5855	1.0000	.0000	1.1964	.0001	.0004	1.0038	.0001	.0003
4.9	4.6855	1.0000	.0000	1.1964	.0001	.0003	1.0038	.0001	.0002
5.0	4.7855	1.0000	.0000	1.1964	.0001	.0002	1.0038	.0000	.0002
5.1	4.8855	1.0000	.0000	1.1964	.0000	.0002	1.0038	.0000	.0001
5.2	4.9855	1.0000	.0000	1.1964	.0000	.0001	1.0038	.0000	.0001
5.3	5.0855	1.0000	.0000	1.1964	.0000	.0001	1.0038	.0000	.0001
5.4	5.1855	1.0000	.0000	1.1964	.0000	.0001	1.0038	.0000	.0000
5.5	5.2855	1.0000	.0000	1.1964	.0000	.0000	1.0038	.0000	.0000

3959

TABLE I. - Continued. LAMINAR BOUNDARY LAYER BEHIND WAVE (EQS. 9 AND 15)

(e) Solution for $u_w/u_e = 2$ (ref. 1)

η	f	f'	f''	Prandtl number σ_w, 0.72					
				$\int_0^\eta r\,d\eta$	r	$-r'$	$\int_0^\eta s\,d\eta$	s	$-s'$
0.0	0.0000	2.0000	-1.0191	0.0000	0.8997	0.0000	0.0000	1.0000	0.8512
.1	.1949	1.8984	-1.0091	.0897	.8922	.1479	.0958	.9151	.8452
.2	.3798	1.7988	-.9804	.1780	.8704	.2861	.1831	.8313	.8279
.3	.5548	1.7029	-.9356	.2634	.8356	.4068	.2621	.7498	.8004
.4	.7205	1.6121	-.8777	.3447	.7898	.5043	.3331	.6715	.7645
.5	.8774	1.5276	-.8103	.4210	.7356	.5758	.3965	.5972	.7217
.6	1.0263	1.4503	-.7367	.4916	.6755	.6209	.4527	.5274	.6739
.7	1.1677	1.3804	-.6601	.5560	.6122	.6412	.5022	.4625	.6227
.8	1.3026	1.3183	-.5834	.6141	.5480	.6398	.5454	.4029	.5697
.9	1.4316	1.2637	-.5088	.6657	.4849	.6206	.5829	.3486	.5162
1.0	1.5556	1.2164	-.4382	.7111	.4244	.5878	.6153	.2996	.4636
1.1	1.6751	1.1759	-.3728	.7507	.3676	.5455	.6430	.2558	.4127
1.2	1.7910	1.1416	-.3135	.7848	.3155	.4974	.6666	.2170	.3643
1.3	1.9036	1.1129	-.2606	.8139	.2683	.4465	.6866	.1829	.3189
1.4	2.0137	1.0893	-.2142	.8386	.2262	.3953	.7034	.1531	.2769
1.5	2.1216	1.0699	-.1742	.8594	.1892	.3456	.7174	.1274	.2386
1.6	2.2278	1.0542	-.1402	.8766	.1570	.2988	.7290	.1053	.2040
1.7	2.3326	1.0417	-.1116	.8909	.1293	.2556	.7385	.0864	.1731
1.8	2.4362	1.0317	-.0879	.9026	.1057	.2166	.7463	.0705	.1458
1.9	2.5390	1.0239	-.0686	.9122	.0858	.1819	.7527	.0572	.1219
2.0	2.6411	1.0179	-.0529	.9199	.0692	.1514	.7578	.0460	.1012
2.1	2.7426	1.0133	-.0404	.9261	.0554	.1250	.7620	.0368	.0833
2.2	2.8438	1.0097	-.0306	.9310	.0441	.1024	.7653	.0293	.0682
2.3	2.9446	1.0071	-.0229	.9350	.0348	.0832	.7679	.0231	.0553
2.4	3.0452	1.0051	-.0170	.9381	.0273	.0671	.7699	.0181	.0446
2.5	3.1456	1.0036	-.0124	.9405	.0213	.0538	.7715	.0141	.0357
2.6	3.2459	1.0026	-.0090	.9424	.0165	.0427	.7728	.0109	.0284
2.7	3.3462	1.0018	-.0065	.9438	.0127	.0337	.7737	.0084	.0224
2.8	3.4463	1.0012	-.0046	.9449	.0097	.0264	.7745	.0064	.0175
2.9	3.5464	1.0008	-.0033	.9458	.0073	.0205	.7750	.0049	.0136
3.0	3.6465	1.0006	-.0023	.9464	.0055	.0158	.7755	.0037	.0105
3.1	3.7465	1.0004	-.0016	.9469	.0041	.0121	.7758	.0028	.0081
3.2	3.8466	1.0003	-.0011	.9473	.0031	.0092	.7760	.0020	.0061
3.3	3.9466	1.0002	-.0007	.9475	.0023	.0070	.7762	.0015	.0046
3.4	4.0466	1.0001	-.0005	.9477	.0017	.0052	.7763	.0011	.0035
3.5	4.1466	1.0001	-.0003	.9479	.0012	.0039	.7764	.0008	.0026
3.6	4.2466	1.0000	-.0002	.9480	.0009	.0029	.7765	.0006	.0019
3.7	4.3466	1.0000	-.0001	.9480	.0006	.0021	.7765	.0004	.0014
3.8	4.4466	1.0000	-.0001	.9481	.0005	.0015	.7766	.0003	.0010
3.9	4.5466	1.0000	-.0001	.9481	.0003	.0011	.7766	.0002	.0007
4.0	4.6466	1.0000	.0000	.9482	.0002	.0008	.7766	.0001	.0005
4.1				.9482	.0002	.0006	.7766	.0001	.0004
4.2				.9482	.0001	.0004	.7766	.0001	.0003
4.3				.9482	.0001	.0003	.7766	.0001	.0002
4.4				.9482	.0001	.0002	.7766	.0000	.0001
4.5				.9482	.0000	.0001	.7767	.0000	.0001
4.6				.9482	.0000	.0001	.7767	.0000	.0001
4.7				.9482	.0000	.0001	.7767	.0000	.0000
4.8				.9482	.0000	.0000	.7767	.0000	.0000
4.9									

3959

TABLE I. - Continued. LAMINAR BOUNDARY LAYER BEHIND SHOCK WAVE (EQS. 9 AND 15)

(f) Solution for $u_w/u_e = 4$ (ref. 1)

η	f	f'	f''	Prandtl number σ_w, 0.72					
				$\int_0^\eta r\,d\eta$	r	$-r'$	$\int_0^\eta s\,d\eta$	s	$-s'$
0.0	0.0000	4.0000	-4.0623	0.0000	0.9129	0.0000	0.0000	1.0000	1.1156
.1	.3798	3.5964	-3.9845	.0909	.8998	.2582	.0945	.8892	1.1005
.2	.7198	3.2077	-3.7702	.1791	.8623	.4847	.1779	.7811	1.0576
.3	1.0222	2.8457	-3.4546	.2626	.8047	.6579	.2509	.6784	.9931
.4	1.2901	2.5188	-3.0766	.3396	.7328	.7690	.3139	.5830	.9136
.5	1.5273	2.2313	-2.6717	.4089	.6529	.8202	.3677	.4960	.8253
.6	1.7377	1.9844	-2.2688	.4701	.5705	.8209	.4134	.4180	.7337
.7	1.9255	1.7768	-1.8887	.5231	.4900	.7838	.4517	.3492	.6429
.8	2.0943	1.6055	-1.5446	.5683	.4145	.7218	.4835	.2893	.5563
.9	2.2476	1.4664	-1.2430	.6062	.3461	.6458	.5098	.2378	.4757
1.0	2.3885	1.3554	-.9858	.6378	.2855	.5646	.5313	.1939	.4026
1.1	2.5195	1.2679	-.7712	.6636	.2331	.4844	.5488	.1570	.3374
1.2	2.6427	1.1998	-.5957	.6846	.1885	.4089	.5629	.1262	.2801
1.3	2.7600	1.1476	-.4547	.7016	.1511	.3406	.5742	.1007	.2306
1.4	2.8727	1.1079	-.3431	.7151	.1201	.2804	.5832	.0798	.1883
1.5	2.9819	1.0781	-.2560	.7258	.0948	.2283	.5903	.0628	.1525
1.6	3.0885	1.0560	-.1890	.7342	.0742	.1842	.5959	.0491	.1226
1.7	3.1933	1.0398	-.1380	.7407	.0577	.1473	.6003	.0382	.0978
1.8	3.2967	1.0280	-.0998	.7458	.0445	.1168	.6036	.0294	.0774
1.9	3.3990	1.0195	-.0714	.7497	.0341	.0919	.6062	.0226	.0608
2.0	3.5006	1.0135	-.0506	.7527	.0260	.0717	.6082	.0172	.0474
2.1	3.6018	1.0092	-.0355	.7550	.0196	.0556	.6097	.0130	.0367
2.2	3.7025	1.0062	-.0246	.7567	.0147	.0427	.6108	.0097	.0282
2.3	3.8030	1.0048	-.0169	.7580	.0110	.0326	.6116	.0073	.0216
2.4	3.9034	1.0028	-.0115	.7589	.0082	.0247	.6123	.0054	.0163
2.5	4.0036	1.0018	-.0077	.7596	.0060	.0186	.6127	.0040	.0123
2.6	4.1038	1.0012	-.0052	.7602	.0044	.0139	.6131	.0029	.0092
2.7	4.2039	1.0008	-.0034	.7605	.0032	.0103	.6133	.0021	.0068
2.8	4.3039	1.0005	-.0022	.7608	.0023	.0076	.6135	.0015	.0050
2.9	4.4040	1.0003	-.0014	.7610	.0016	.0055	.6136	.0011	.0037
3.0	4.5040	1.0002	-.0009	.7611	.0012	.0040	.6137	.0008	.0027
3.1	4.6040	1.0001	-.0006	.7612	.0008	.0029	.6138	.0005	.0019
3.2	4.7040	1.0001	-.0004	.7613	.0006	.0021	.6138	.0004	.0014
3.3	4.8040	1.0001	-.0002	.7613	.0004	.0015	.6139	.0003	.0010
3.4	4.9040	1.0000	-.0001	.7614	.0003	.0010	.6139	.0002	.0007
3.5	5.0040	1.0000	-.0001	.7614	.0002	.0007	.6139	.0001	.0005
3.6	5.1040	1.0000	-.0001	.7614	.0001	.0005	.6139	.0001	.0003
3.7	5.2040	1.0000	.0000	.7614	.0001	.0003	.6139	.0001	.0002
3.8				.7614	.0001	.0002	.6139	.0000	.0002
3.9				.7614	.0000	.0002	.6139	.0000	.0001
4.0				.7614	.0000	.0001	.6139	.0000	.0001
4.1				.7615	.0000	.0001	.6139	.0000	.0000
4.2				.7615	.0000	.0000	.6139	.0000	.0000
4.3									
4.4									

3959

TABLE I. - Concluded. LAMINAR BOUNDARY LAYER BEHIND SHOCK WAVE (EQS. 9 AND 15)

(g) Solution for $u_w/u_e = 6$ (ref. 1)

η	f	f'	f''	Prandtl number σ_w, 0.72					
				$\int_0^\eta r\,d\eta$	r	$-r'$	$\int_0^\eta s\,d\eta$	s	$-s'$
0.0	0.0000	6.0000	-8.1009	0.0000	0.9195	0.0000	0.0000	1.0000	1.3262
.1	.5597	5.1977	-7.8721	.0913	.9009	.3658	.0934	.8683	1.2991
.2	1.0410	4.4383	-7.2620	.1791	.8486	.6668	.1738	.7417	1.2258
.3	1.4499	3.7534	-6.4078	.2602	.7710	.8671	.2420	.6242	1.1202
.4	1.7947	3.1603	-5.4454	.3328	.6787	.9619	.2991	.5183	.9963
.5	2.0852	2.6643	-4.4831	.3958	.5816	.9681	.3461	.4252	.8662
.6	2.3307	2.2613	-3.5937	.4492	.4871	.9118	.3845	.3450	.7387
.7	2.5402	1.9418	-2.8161	.4935	.4004	.8187	.4155	.2771	.6197
.8	2.7214	1.6938	-2.1642	.5296	.3239	.7094	.4403	.2206	.5127
.9	2.8809	1.5048	-1.6353	.5586	.2586	.5983	.4600	.1742	.4190
1.0	3.0240	1.3631	-1.2171	.5817	.2040	.4941	.4755	.1364	.3388
1.1	3.1548	1.2583	-.8935	.5998	.1594	.4012	.4875	.1060	.2712
1.2	3.2766	1.1818	-.6478	.6138	.1234	.3212	.4969	.0818	.2151
1.3	3.3918	1.1266	-.4641	.6247	.0947	.2542	.5040	.0626	.1692
1.4	3.5024	1.0873	-.3288	.6330	.0721	.1991	.5095	.0476	.1320
1.5	3.6097	1.0597	-.2304	.6393	.0545	.1545	.5137	.0360	.1022
1.6	3.7146	1.0403	-.1597	.6440	.0409	.1189	.5168	.0270	.0785
1.7	3.8180	1.0270	-.1096	.6476	.0305	.0908	.5192	.0201	.0599
1.8	3.9202	1.0179	-.0744	.6502	.0226	.0687	.5209	.0149	.0453
1.9	4.0217	1.0118	-.0500	.6521	.0166	.0517	.5222	.0109	.0340
2.0	4.1226	1.0077	-.0333	.6536	.0121	.0385	.5231	.0080	.0254
2.1	4.2232	1.0049	-.0219	.6546	.0088	.0285	.5238	.0058	.0188
2.2	4.3236	1.0031	-.0143	.6554	.0063	.0210	.5243	.0042	.0138
2.3	4.4239	1.0020	-.0092	.6559	.0045	.0153	.5246	.0030	.0101
2.4	4.5240	1.0012	-.0059	.6563	.0032	.0111	.5249	.0021	.0073
2.5	4.6241	1.0008	-.0037	.6565	.0023	.0080	.5251	.0015	.0053
2.6	4.7242	1.0005	-.0023	.6567	.0016	.0057	.5252	.0010	.0038
2.7	4.8242	1.0003	-.0015	.6569	.0011	.0040	.5253	.0007	.0027
2.8	4.9243	1.0002	-.0009	.6570	.0008	.0028	.5253	.0005	.0019
2.9	5.0243	1.0001	-.0005	.6570	.0005	.0020	.5254	.0003	.0013
3.0	5.1243	1.0001	-.0003	.6571	.0004	.0014	.5254	.0002	.0009
3.1	5.2243	1.0000	-.0002	.6571	.0002	.0010	.5254	.0002	.0006
3.2	5.3243	1.0000	-.0001	.6571	.0002	.0007	.5254	.0001	.0004
3.3	5.4243	1.0000	-.0001	.6571	.0001	.0004	.5255	.0001	.0003
3.4	5.5243	1.0000	.0000	.6571	.0001	.0003	.5255	.0000	.0002
3.5				.6572	.0000	.0002	.5255	.0000	.0001
3.6				.6572	.0000	.0001	.5255	.0000	.0001
3.7				.6572	.0000	.0001	.5255	.0000	.0001
3.8				.6572	.0000	.0001	.5255	.0000	.0000
3.9				.6572	.0000	.0000	.5255	.0000	.0000

3959

TABLE II. - COMPARISON OF INTEGRAL METHOD WITH EXACT INTEGRATION OF EQUATION (9)

	u_w/u_e					
	0		1		6	
	Eq. (9)	Eq. (23)	Eq. (9)	Eq. (23)	Eq. (9)	Eq. (23)
$\frac{f''(0)}{1 - (u_w/u_e)}$	0.4696	0.4847	0.7979	0.7746	1.6202	1.5574
$\lim_{\eta \to \infty} \frac{\eta - f}{1 - (u_w/u_e)}$	1.2168	1.2379	0.7979	0.7746	0.4249	0.3853

TABLE III. - COMPARISON OF INTERPOLATION FORMULAS WITH EXACT INTEGRATIONS OF EQUATIONS (9) AND (15)(PRANDTL NUMBER σ_w, 0.72)

	u_w/u_e									
	0.25		0.50		0.75		2.0		4.0	
	Eqs. (9), (15)	Eq. (27)	Eqs. (9), (15)	Eq. (27)	Eqs. (9), (15)	Eq. (27)	Eqs. (9), (15)	Eq. (27)	Eqs. (9), (15)	Eq. (27)
$\frac{f''(0)}{1 - (u_w/u_e)}$	0.5727	0.570	0.6574	0.655	0.7312	0.730	1.0191	1.017	1.3541	1.353
$\lim_{\eta \to \infty} \frac{\eta - f}{1 - (u_w/u_e)}$	1.0448	1.054	0.9360	0.944	0.8580	0.862	0.6466	0.650	0.5013	0.503
$\int_0^\infty r\, d\eta$	1.3970	1.396	1.2822	1.279	1.1964	1.194	0.9482	0.940	0.7615	0.754
$\int_0^\infty s\, d\eta$	1.1974	1.201	1.0854	1.087	1.0038	1.004	0.7767	0.774	0.6139	0.610
$-s'(0)$	0.4996	0.502	0.5665	0.569	0.6247	0.627	0.8512	0.856	1.1156	1.122
$r(0)$	0.8628	0.858	0.8727	0.867	0.8799	0.876	0.8997	0.893	0.9129	0.907

TABLE IV. - RECIPROCALS OF INTEGRALS OCCURRING IN TURBULENT-BOUNDARY-LAYER ANALYSIS

(a) Reciprocal of I_6 (based on numerical results of ref. 11)

$\frac{c}{b+1}$	b										
	-1.0	-.8	-.6	-.4	-.2	0	2	4	6	8	10
0	0	1.958	3.270	4.531	5.770	6.998	19.07	31.00	42.96	54.88	66.84
.100		1.830	3.036	4.193	5.328	6.452	17.49	28.43	39.34	50.13	61.05
.200		1.700	2.799	3.851	4.883	5.900	15.92	25.83	35.74	45.62	55.46
.300		1.567	2.557	3.503	4.427	5.342	14.31	23.19	32.06	40.90	49.70
.400		1.430	2.310	3.149	3.967	4.776	12.70	20.54	28.39	36.17	43.94
.500		1.288	2.056	2.784	3.495	4.196	11.06	17.84	24.63	31.43	38.02
.600		1.139	1.792	2.410	3.011	3.604	9.390	15.11	20.79	26.52	32.28
.700		.9814	1.516	2.019	2.507	2.988	7.680	12.29	16.91	21.52	26.06
.750		.8969	1.370	1.814	2.244	2.716	6.789	10.86	14.89	18.91	23.02
.800		.8071	1.217	1.599	1.970	2.334	5.869	9.363	12.84	16.31	19.80
.850		.7097	1.054	1.372	1.682	1.983	4.921	7.831	10.70	13.58	16.44
.900		.5995	.8726	1.123	1.366	1.603	3.897	6.150	8.410	10.63	12.86
.950		.4575	.6418	.8285	.9960	1.161	2.738	4.288	5.865	7.391	8.945
.975		.3469	.5003	.6317	.7559	.8764	2.027	3.151	4.270	5.397	6.527
1.000		0	0	0	0	0	0	0	0	0	0

(b) Reciprocal of I_7 (based on numerical results of ref. 11)

$\frac{c}{b+1}$	b										
	-1.0	-.8	-.6	-.4	-.2	0	2	4	6	8	10
0	0	2.175	3.683	5.142	6.581	8.009	22.12	36.16	50.18	64.20	78.21
.100		2.027	3.411	4.746	6.061	7.366	20.25	33.06	45.85	58.64	71.43
.200		1.879	3.135	4.345	5.536	6.717	18.36	29.94	41.50	53.06	64.62
.300		1.726	2.855	3.940	5.006	6.062	16.47	26.81	37.13	47.45	57.77
.400		1.570	2.570	3.528	4.468	5.398	14.56	23.65	32.73	41.80	50.88
.500		1.409	2.278	3.107	3.920	4.724	12.62	20.46	28.28	36.10	43.92
.600		1.240	1.976	2.675	3.359	4.034	10.66	17.22	23.78	30.32	36.87
.700		1.062	1.660	2.226	2.778	3.322	8.643	13.91	19.17	24.43	29.68
.750		.9672	1.495	1.992	2.476	2.952	7.609	12.22	16.82	21.41	26.01
.800		.8668	1.322	1.748	2.163	2.571	6.548	10.48	14.41	18.33	22.25
.850		.7584	1.138	1.491	1.854	2.170	5.447	8.685	11.91	15.14	18.37
.900		.6360	.9350	1.211	1.478	1.739	4.278	6.783	9.282	11.78	14.27
.950		.4805	.6924	.8826	1.064	1.243	2.965	4.662	6.354	8.044	9.733
.975		.3606	.5247	.6657	.7987	.9279	2.165	3.381	4.593	5.804	7.014
1.000		0	0	0	0	0	0	0	0	0	0

(c) Reciprocal of I_8 (based on numerical results of ref. 11)

$\frac{c}{b+1}$	b										
	-1.0	-.8	-.6	-.4	-.2	0	2	4	6	8	10
0	0	2.388	4.092	5.744	7.380	9.001	25.11	41.17	57.18	73.21	89.21
.100		2.221	3.781	5.294	6.784	8.264	22.95	37.57	52.16	66.76	81.37
.200		2.054	3.467	4.836	6.184	7.519	20.76	33.96	47.10	60.28	73.42
.300		1.882	3.149	4.373	5.574	6.770	18.58	30.33	42.07	53.82	65.53
.400		1.707	2.827	3.905	4.963	6.010	16.38	26.69	36.98	47.26	57.57
.500		1.527	2.496	3.425	4.338	5.241	14.15	23.00	31.85	40.68	49.50
.600		1.338	2.156	2.936	3.701	4.456	11.90	19.28	26.67	34.03	41.41
.700		1.140	1.801	2.430	3.043	3.650	9.597	15.48	21.38	27.26	33.13
.750		1.035	1.617	2.166	2.703	3.231	8.418	13.56	18.68	23.80	28.94
.800		.9242	1.424	1.893	2.351	2.801	7.210	11.57	15.93	20.28	24.64
.850		.8045	1.219	1.606	1.983	2.352	5.963	9.542	13.09	16.66	20.22
.900		.6711	.9950	1.295	1.586	1.871	4.645	7.386	10.12	12.86	15.58
.950		.5023	.7294	.9337	1.129	1.322	3.179	5.010	6.840	8.666	10.49
.975		.3734	.5473	.6974	.8389	.9766	2.296	3.592	4.885	6.177	7.468
1.000		0	0	0	0	0	0	0	0	0	0

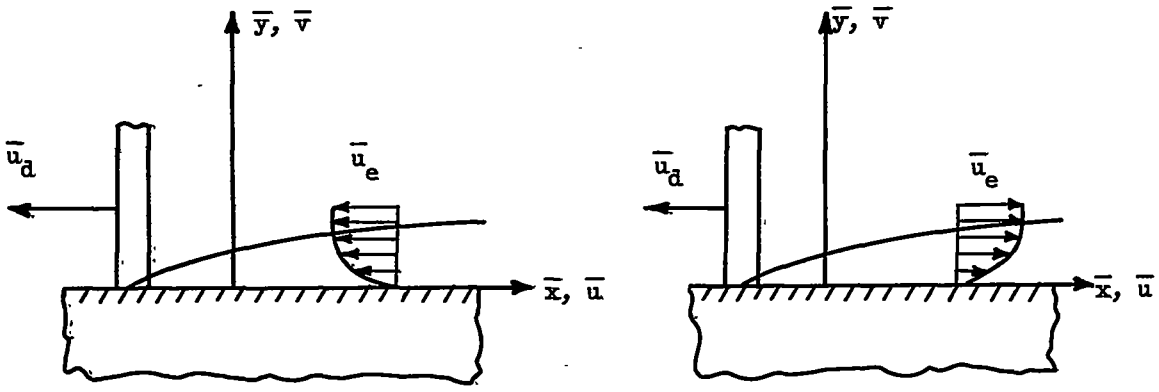

Shock wave Expansion wave

(a) With respect to wall.

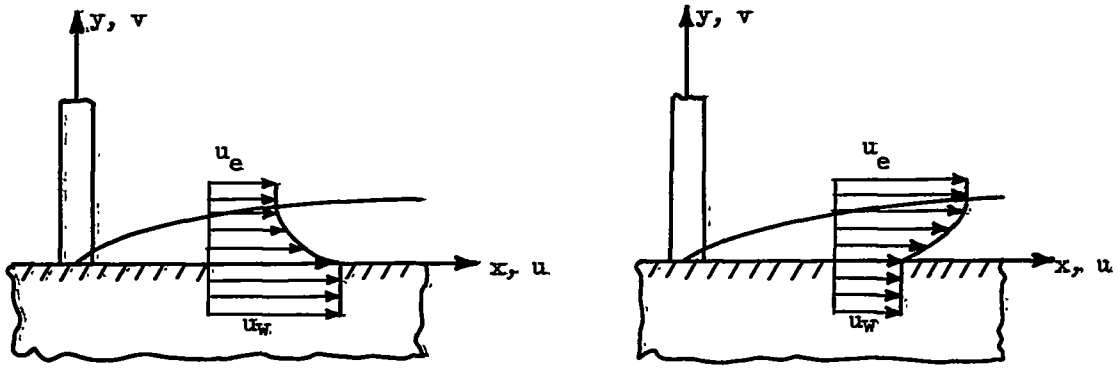

Shock wave Expansion wave

(b) With respect to wave.

Figure 1. - Coordinate systems used to study boundary layer behind a wave advancing into a stationary fluid.

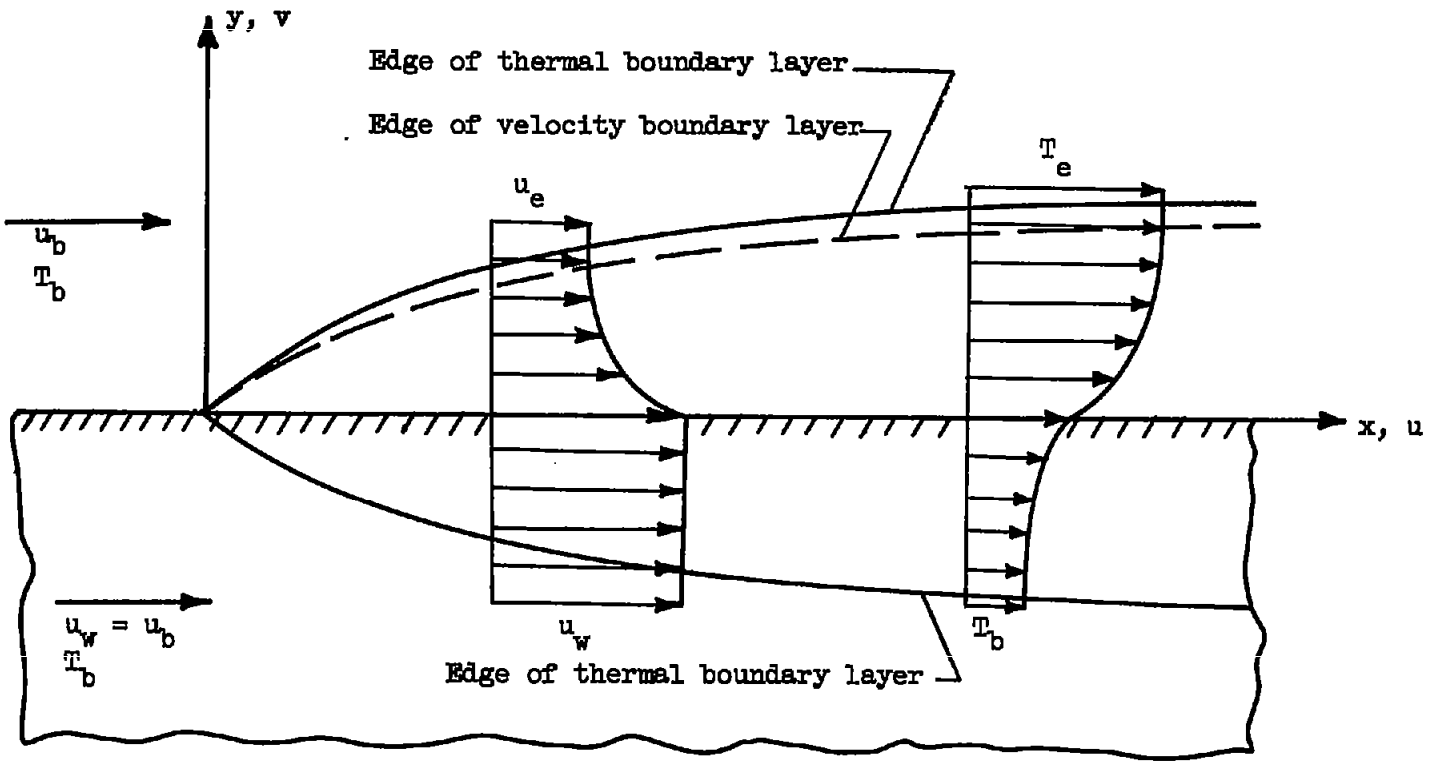

Figure 2. - Temperature and velocity distributions behind a shock wave.

NACA - Langley Field, Va.